DALHOUSIE UNIVERSITY

COMPOUND SPECIFIC ISOTOPE ANALYSIS OF MUSSEL (*MYTILUS EDULIS*) TISSUES: DETERMINING SOURCES OF NITROGEN IN COASTAL NOVA SCOTIA

Rachel Noddle

SUBMITTED IN PARTIAL FULFILLMENT OF THE REQUIREMENTS FOR
THE DEGREE OF BACHELOR OF SCIENCES, HONOURS
DEPARTMENT OF EARTH SCIENCES
DALHOUSIE UNIVERSITY, HALIFAX, NOVA SCOTIA

April 2020

DALHOUSIE UNIVERSITY

Department of Earth Sciences
Halifax, Nova Scotia
Canada B3H 4R2
(902) 494-2358

DATE: 03/30/2020

AUTHOR: Rachel Noddle

TITLE: Compound Specific Isotope Analysis of Invertebrate Tissues: Determining Nitrogen Variability in Coastal Nova Scotia

DEGREE: Bachelor of Science CONVOCATION: May YEAR: 2020

Distribution License

DalSpace requires agreement to this non-exclusive distribution license before your item can appear on DalSpace.

NON-EXCLUSIVE DISTRIBUTION LICENSE

You (the author(s) or copyright owner) grant to Dalhousie University the non-exclusive right to reproduce and distribute your submission worldwide in any medium.

You agree that Dalhousie University may, without changing the content, reformat the submission for the purpose of preservation.

You also agree that Dalhousie University may keep more than one copy of this submission for purposes of security, back-up and preservation.

You agree that the submission is your original work, and that you have the right to grant the rights contained in this license. You also agree that your submission does not, to the best of your knowledge, infringe upon anyone's copyright.

If the submission contains material for which you do not hold copyright, you agree that you have obtained the unrestricted permission of the copyright owner to grant Dalhousie University the rights required by this license, and that such third-party owned material is clearly identified and acknowledged within the text or content of the submission.

If the submission is based upon work that has been sponsored or supported by an agency or organization other than Dalhousie University, you assert that you have fulfilled any right of review or other obligations required by such contract or agreement.

Dalhousie University will clearly identify your name(s) as the author(s) or owner(s) of the submission, and will not make any alteration to the content of the files that you have submitted.

If you have questions regarding this license please contact the repository manager at dalspace@dal.ca.

Grant the distribution license by signing and dating below.

Rachel Noddle	March 30, 2020
Name of signatory	Date

Contents

List of Figures

List of Tables

Acknowledgements

I would like to thank Dr. Owen Sherwood and the rest of Dalhousie's Stable Isotope Biogeochemical Laboratory for their continued patience, support, and guidance throughout this project. It is through their appreciation and dedication to stable isotope ecology that has made this project possible. My sincerest gratitude is extended to Bay Berry and Katie Frame for sample collection, Chelsea Fougere and Blake Tibert for CSIA preparation and analysis, Claire Normandeau for bulk isotope analysis, Liz Kerrigan for nutrient analysis, Shaomin Chen for help with PCA analysis, and Nina Golombek for decoding Latex. Thank you.

Abstract

Anthropogenic nitrogen (N) loading in coastal marine environments causes eutrophication, alters food web structures, and degrades water quality. In Nova Scotia, anthropogenic N sources are introduced to coastal waters through multiple sources including sewage wastewater outfalls, seafood processing, aquaculture, and agricultural runoff. Different N sources have characteristic isotopic (δ^{15}N) signatures that can be traced using bioindicator organisms to map the spatial variability of δ^{15}N along the coastline. Organisms such as the blue mussel *(Mytilus edulis)* integrate the isotopic δ^{15}N composition of their local environment by feeding on particulate organic matter and integrating it into their tissues over several months. Mussels are ideal bio-indicators for this study because they are sessile organisms that are found along the rocky intertidal zone of the province's coastline, preserving the biogeochemical variability of their collection sites. This allows us to map the spatial variability of δ^{15}N to help identify sources of N in a region with few previous N measurements.

Specimens of *M. edulis* were collected in triplicate from 21 sites across the province's Atlantic and Northumberland coasts. The adductor muscle of *M. edulis* was isolated from the rest of the tissue, removed, and freeze-dried for δ^{15}N analysis. Within-site variability was considerably low (mean of standard deviation = 0.56 ‰), indicating narrow variability within specimens at each site. There was, however, a wide range of mean δ^{15}N values between sites, ranging from 6.80 ± 0.27 ‰ to 11.08 ± 1.00 ‰ (n=21). To refine these baseline δ^{15}N estimates independent of trophic fractionation, 8 sites with the largest δ^{15}N ranges were selected for compound specific isotope analysis (CSI-AA). Amino acids were isolated for δ^{15}N analysis through acid hydrolysis, cation exchange and isopropyl TFAA derivatization. Individual amino acid values ranged from -7.5 ‰ to 18.1 ‰ (SD=5.5; n=250). Phenylalanine (Phe) is the best amino acid proxy for baseline δ^{15}N Phe values and ranged from 2.4 ± 1.2 ‰ to 7.8 ± 0.9 ‰; n=22. This variability reflects similar trends in the bulk

δ^{15}N values, indicating that the local variability seen in *M. edulis* δ^{15}N likely reflects inputs of different nitrogen sources specific to each sample site. This study pairs the novel CSI-AA approach with traditional nutrient data and bulk δ^{15}N analysis to generate estimates of baseline δ^{15}N variability for the Northumberland and Atlantic coasts of Nova Scotia.

1 Introduction

1.1 Motivation

Anthropogenic nutrient pollution poses a global threat to the health and biodiversity of coastal marine ecosystems. Input of excess nitrogen (N) from human activities can cause eutrophication, alter foodweb structures, and degrade water quality (Diaz & Rosenberg, 2008; Conley *et al.* , 2009). Eutrophication has caused the exponential increase of dead zones within coastal ecosystems since the 1960s, affecting more than 245,000 km^2 worldwide (Diaz & Rosenberg, 2008). With a ∼7600 km coastline, Nova Scotia is home to one of Canada's most ecologically productive and diverse bioregions which stimulates approximately $4.5 billion dollars in the province's ocean-related industries (Bernier & Moore, 2018; Gardner *et al.* , 2005). In Nova Scotia, eutrophication is of growing concern because anthropogenic N is introduced to coastal waters through multiple sources, including sewage wastewater outfalls, seafood processing, aquaculture, and agricultural runoff (McIver *et al.* , 2018; Nagel *et al.* , 2018; Fowler *et al.* , 2013).

Stable nitrogen isotopes (δ^{15}N) have proven to be a useful tool in distinguishing among different sources of nitrogen in coastal settings (Costanzo *et al.* , 2001; McClelland *et al.* , 1997; Vander Zanden *et al.* , 2005). This is because different N sources have characteristic isotopic (δ^{15}N) signatures, which are incorporated into the tissues of organisms that inhabit the local environment (Peterson & Fry, 1987). Organisms such as the filter-feeding Blue Mussel (*Mytilus edulis*) feed on particulate organic matter integrating these isotopic δ^{15}N signatures into their tissues, preserving the biogeochemical variability of the base of the marine foodweb over periods of several months (Widdows *et al.* , 1979; Cabana & Rasmussen, 1996). The goal of this project is to determine the spatial variability of δ^{15}N at the base of the marine foodweb, using specimens of *M. edulis*, to better understand inputs of anthropogenic nitrogen to coastal Nova Scotia.

1.2 Background

1.2.1 Environmental Setting

Nova Scotia is one of Canada's eastern-most provinces, located between 43°N and 47°N. This peninsula has a marine coastline bordered by the Bay of Fundy, the Gulf of the St. Lawrence, and the open North-west Atlantic. Each coastline has unique temperature, salinity, and tidal characteristics, summarized below.

The Bay of Fundy is a funnel-shaped inlet that is over 270km long and 60km at it's widest point, separating Nova Scotia from New Brunswick and the State of Maine (Bernier & Moore, 2018). Known for it's high tidal range, the upwelling that occurs in the Bay of Fundy is caused by the interaction between the warm Gulf current and cold North Atlantic tides (Gran & Braarud, 1935). This macrotidal environment is home to a diverse array of biological productivity, however, the strong tides and high silt content create unsuitable habitat for *M. edulis* (Garrett, 1972; Dalrymple *et al.* , 1978).

On Nova Scotia's southern shores, the cold Labrador current descends along the Atlantic flushing the hundreds of small embayments that indent the Atlantic coastline (Strain & Yeats, 1999). Offshore, seasonal upwelling driven by tidal forces, wind stress and circulation-associated with being adjacent to deep-ocean gyres creates nutrient-rich waters (Smith & Schwing, 1991).

The Northumberland Strait comprises the southern part of the Gulf of the St. Lawrence, formed between Prince Edward Island, New Brunswick, and Nova Scotia. This shallow coastline is 68m at it's deepest point on the eastern edge of the strait, but is 20m throughout much of the central region (Kranck, 1972b). These shallow waters lend themselves to strong tidal currents that suspend the red sandstone and siltstone exposed at the bottom of the strait (Kranck, 1972b). Strong tidal currents promote elevated nutrient concentrations and create conditions that are favourable

for primary productivity (Kranck, 1972a).

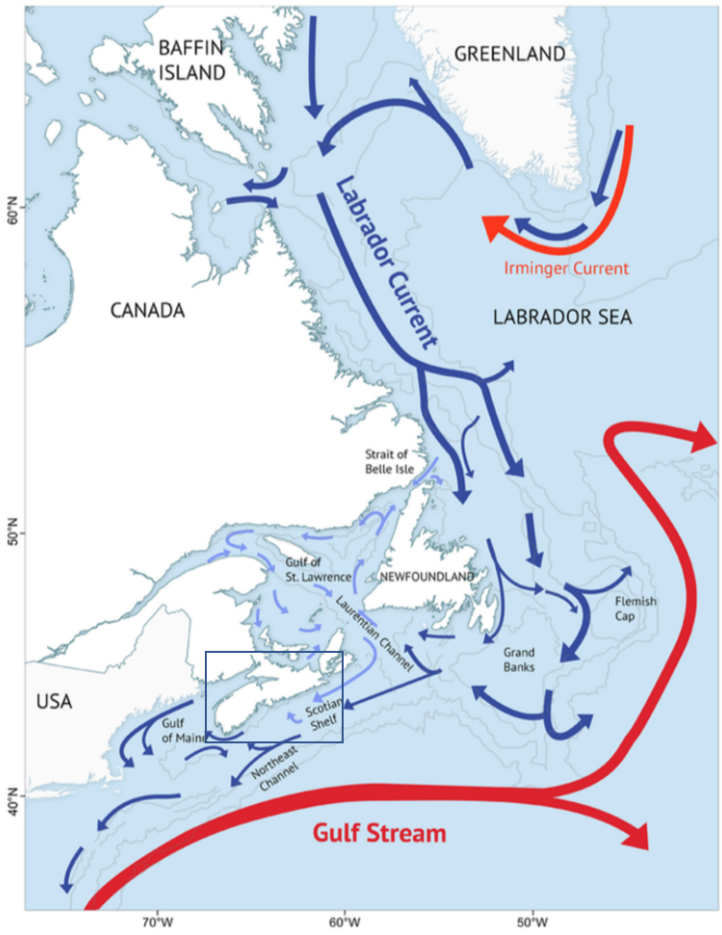

Figure 1: Map illustrating the currents of Atlantic Canada. There are two main current systems that influence the region: the cold Labrador current from the North (blue) and the warm Gulf Stream from the South (red) (Bernier & Moore, 2018). The study area is denoted by the rectangle.

Nova Scotia has a rich geologic history that informs present day biogeochemical nutrient behaviour. The Laurentide ice sheet covered Nova Scotia for the duration of the Pliestocene, before it's eventual retreat between 18 to 13 ka (Dyke & Prest, 1987). The isostatic recovery of Nova Scotia, postglacial sedimentation, and erosion from 13 ^{14}C kyr BP onward has led to the creation of unique morphological features seen within this indented coastline today (Shaw *et al.* , 2002). Nova Scotia's coastline is home to hundreds of small embayments that were created by basins that have been carved by glaciers, followed by more recent deposition of silt (Dyke & Prest,

1987; Kranck, 1972a). The combination of these geologic processes lend itself to the creation of many silled basins and this morphology plays an important role in the nitrogen cycle because it creates hundreds of poorly circulating basins (Strain & Yeats, 1999). The poor circulation promotes periodically suboxic bottom water conditions, which can promote denitrificaiton (Strain & Yeats, 1999; Haas & Wallace, 2020).

1.2.2 Understanding Nutrient Sources

The marine nitrogen cycle is one of the fundamental biogeochemical cycles, comprising transformations of the various forms of fixed nitrgoen (i.e. Ammonium, Nitrate, Nitrite)(Francis *et al.* , 2005; Gruber & Sarmiento, 1997). The bioavailable form of nitrogen (primarily nitrate), is a critical component of the ocean because it is often diminished before phosphorus, thus setting the upper limit of primary production (Falkowski, 1997). Nitrogenous transformations, such as N_2 fixation, annamox and denitrification, are mediated by microogranisms which are responsible for the major source and sink processes of the N cycle (Dalsgaard *et al.* , 2005; Sohm *et al.* , 2011). Sources of N to the marine environment include fixation of atmospheric N_2 gas by diazotrophs, atmospheric deposition, and land-based runoff of natural and anthropogenic nutrients (e.g., Dalsgaard *et al.* , 2005; Sohm *et al.* , 2011). The primary sinks of marine N are water column and sedimentary denitrification (Gruber & Sarmiento, 1997). The global nitrogen budget that dictates these source and sink processes is currently being perturbed through the addition of anthropogenic sources such as sewage wastewater outfalls, seafood processing, aquaculture, and agricultural runoff (e.g., Costanzo *et al.* , 2001; Yokoyama *et al.* , 2006).

Detecting anthropogenic N sources in the ocean is challenging because many water quality assessment tools, such as ambient nutrient uptake and salinity measurements, are ineffective in dynamic coastal environments (e.g., Šraj *et al.* , 2014). Locations with potentially elevated nutrient levels can be rapidly diluted by currents, wave action and general mixing events (Deborde *et al.* , 2008). In addition,

biological N uptake rates may closely resemble the rates of N input, making detection of nutrient fluxes quite difficult (Wheeler & Kirchman, 1986; Ryan *et al.* , 2008a).

1.2.3 Bulk Isotope Analysis

Stable isotope analysis is widely used within ecological studies because it provides detailed nuanced views of element cycling within dynamic systems (Fry, 2006). The following section outlines bulk nitrogen and carbon isotope analysis, as well as introducing the novel compound-specific isotope analysis approach this study used to trace nitrogen variability within coastal Nova Scotia.

1.2.4 Nitrogen Isotopes

Nitrogen has two stable isotopes, ^{14}N and ^{15}N (denoted by their respective atomic masses, 14 and 15). ^{14}N is the more abundant of the two, which comprise of 99.63% of nitrogen found in the biosphere (Sigman *et al.* , 2009). Chemical, physical, and biological fractionation processes lead to subtle but measurable differences in the ratio of ^{14}N and ^{15}N found in the ocean (Peterson & Fry, 1987). Isotopic results are expressed in parts per thousand (‰) as δ^{15}N based on the following:

$$\delta^{15}N = [\frac{^{15}N/^{14}N_{Sample}}{^{15}N/^{14}N_{Standard}} - 1] \times 1000 \quad (1)$$

where atmospheric air is the universal standard. Nitrogen isotopes experience both equilibrium and kinetic fractionation within the ocean (Fry, 2006). δ^{15}N variations in the marine N cycle are dominated by kinetic fractionation associated with the conversion of N forms (i.e. nitrate to nitrite) (e.g., Wada & Hattori, 1978; Checkley Jr & Miller, 1989). Primary producer organisms (e.g. microalgae, seaweeds, seagrasses) discriminate against ^{15}N during assimilation of nitrate and ammonium, following Rayleigh fractionation kinetics (Mariotti *et al.* , 1982; Wada & Hattori, 1978; Needoba *et al.* , 2003). Heterotrophic organisms also fractionate N isotopes

during metabolic processing, lending to step-wise increase in δ^{15}N through successive trophic levels (DeNiro & Epstein, 1981; Wada & Hattori, 1978). This trophic fractionation factor averages approximately 3.4‰ (DeNiro & Epstein, 1981; Fry, 2006). Nitrogenous transformations throughout the ocean are complex and as a limiting element for biological productivity, nitrogen furthers that complexity through it's influence on other biogeochemical cycles such as the carbon cycle (Gruber, 2004).

1.2.5 Carbon Isotopes

Carbon also has two stable isotopes, ^{13}C and ^{12}C (denoted by their atomic masses, 13 and 12). The respective abundances of ^{13}C and ^{12}C are 98.89% and 1.11% in the world (Craig, 1953). Carbon isotopes are defined by:

$$\delta^{13}C = [\frac{^{13}C/^{12}C_{Sample}}{^{13}C/^{12}C_{Standard}} - 1] \times 1000 \quad (2)$$

where the universal standard is Vienna Pee Dee Belemnite (VPDB) standard reported in per mil (Coplen, 1996). Trophic fractionation of carbon isotopes is small relative to that of nitrogen (∼1 ‰) (DeNiro & Epstein, 1978). In coastal ecosystems, δ^{13}C is often interpreted as a proxy for terrestrial (δ^{13}C ∼ 26 ‰) versus marine (δ^{13}C ∼ 20 ‰) sources of carbon (Fry, 2006; LeBlanc *et al.* , 1989; Tan & Strain, 1979). Carbon isotopes are used to compliment nitrogen isotopic (δ^{15}N) data within this study to gain a better understanding of the behaviour of N sources in the coastal zone.

1.2.6 Isotopic Nutrient Signatures

Stable nitrogen isotope analysis has proven to be an effective tool used to identify nitrogen sources in coastal aquatic ecosystems, as illustrated in Figure 2 (Costanzo *et al.* , 2001; McClelland *et al.* , 1997; Vander Zanden *et al.* , 2005). This is attributed to the fact that different N sources have unique isotopic signatures and anthropogenic N sources are often distinguished from most natural sources of dissolved organic nitrogen (DIN) (e.g., Owens, 1988; Heaton, 1986). For example, the

δ^{15}N of atmospheric N_2 is 0 ‰ by definition (Peterson & Fry, 1987). Newly fixed N by diazotrophs has a δ^{15}N of -3 to 0 ‰(Owens, 1988). Global mean nitrate from deep seawater is approximately 3-5 ‰ (Sigman *et al.* , 2000). This is contrasted by the isotopically enriched signature of sewage wastewater, which has a δ^{15}N value of 10+ ‰ (Heaton, 1986). Other anthropogenic inputs, like the dissolved wastes derived from salmon aquaculture have δ^{15}N values of 8-11 ‰ (García-Sanz *et al.* , 2010). These unique isotopic signatures continue to be used globally to asses N sources to coastal marine ecosystems (e.g., Vokhshoori & McCarthy, 2014; Costanzo *et al.* , 2001).

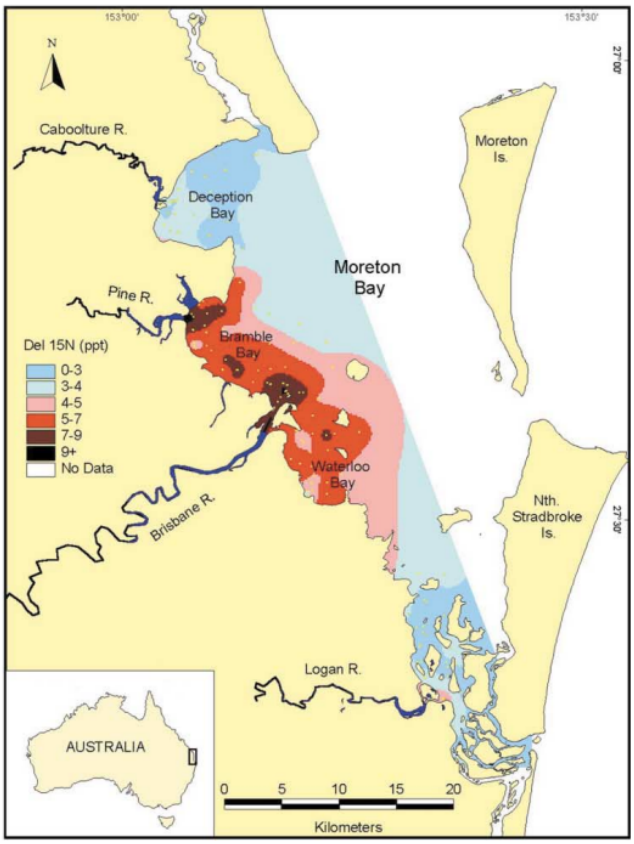

Figure 2: Isoscape of macroalgal δ^{15}N values in Moreton Bay Australia for detecting and mapping sewage outfalls (Costanzo *et al.* , 2001).

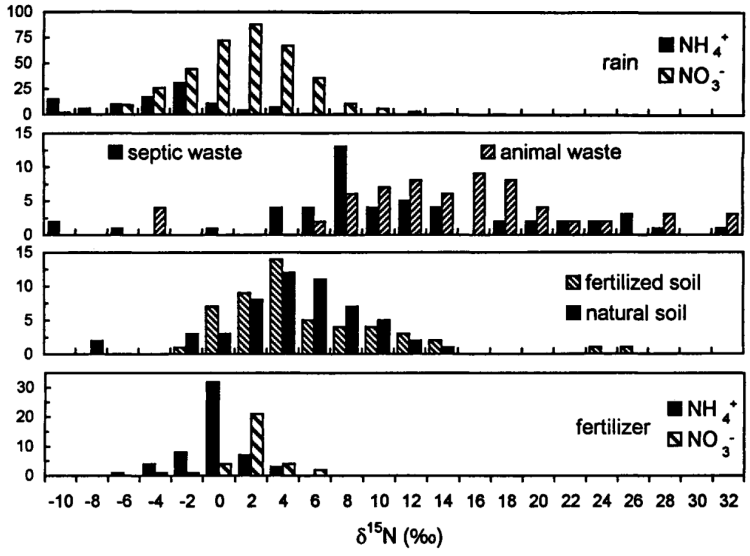

Figure 3: Summary of the δ^{15}N values of the major nitrogen sources in the hydrosphere, from Kendall (1998).

1.2.7 Compound-Specific Isotope Analysis

Bulk δ^{15}N isotopic analysis has been widely used in ecological studies to understand nitrogen's behaviour in oceanographic, terrestrial, and freshwater systems (e.g., Owens, 1988; Wada *et al.* , 1975; Fry, 2006). The primary caveat with the bulk isotopic analysis of nitrogen, however, is that it measures all nitrogen entities within a sample, making the interpretation of bulk δ^{15}N data quite challenging. This is because independent factors such as trophic transfer and microbial degradation can influence bulk δ^{15}N data, making it difficult to differentiate from the δ^{15}N isotopic baseline(McCarthy *et al.* , 2007; Ohkouchi *et al.* , 2017)

Compound-specific isotope analysis of amino acids (CSIA-AA) is an emerging technique that can address some of the inherent problems associated with bulk δ^{15}N analysis (McMahon *et al.* , 2015; Ohkouchi *et al.* , 2017). The seminal paper by McClelland & Montoya (2002) paved the way for CSIA-AA work by demonstrating that some amino acids (AAs) reflect changes in ^{15}N from food source to consumer, while other AAs show no δ^{15}N change with trophic transfer and therefore preserve information about nitrogen sources at the base of the marine foodweb (McClelland & Montoya, 2002). The AAs that show strong differential ^{15}N enrichment associated with each trophic transfer ($\sim$ 4-8‰) are termed the "Trophic AAs" (McClelland & Montoya, 2002; Chikaraishi *et al.* , 2009). These AAs undergo transamination reactions during metabolic processing, which causes isotopic fractination (Macko *et al.* , 1986). The second group of AAs show little to no change in δ^{15}N content through trophic transfer because N bonds are not broken during metabolic processing (Figure 4). These "Source AAs" therefore act as a proxy for understanding the sources of anthropogenic nitrogen in aquatic foodwebs (McClelland & Montoya, 2002). This differential AA enrichment pattern has now been proven among a variety of consumers, with previous CSIA-AA work suggesting that when applied to the appropriate heterotrophic organisms, the $\delta^{15}N_{AA}$ enrichment can indicate baseline δ^{15}N independent of trophic level changes (Vokhshoori & McCarthy, 2014; Ohkouchi

et al. , 2017; Sherwood *et al.* , 2011).

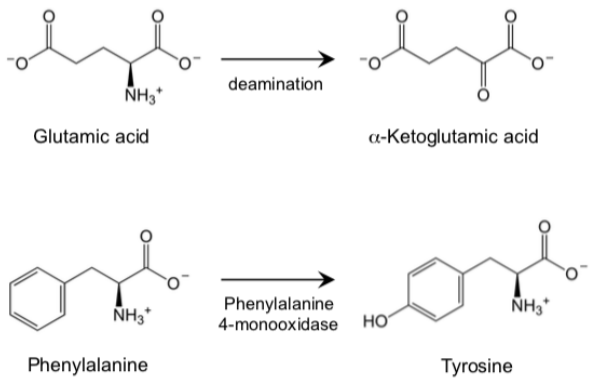

Figure 4: Schematic illustration of differences in "Trophic" and "Source" AA metabolism from Chikaraishi *et al.* (2009). Trophic AAs (e.g. Glutamic acid) undergo a deamination reaction where N bonds are broken during conversion to keto-acids, resulting in N isotope fractionation. Source AAs (e.g. Phenylalanine) do not undergo transamination reactions, and therefore no breaking of N bonds.

The term *isoscape* refers to a map of the spatial distribution of baseline isotope variability (West *et al.* , 2009; Bowen, 2010). Isoscapes have become increasingly useful in many ecological studies because they represent a new approach to understanding regional biogeochemical processes, as shown in Figure 5 (e.g., Graham *et al.* , 2010; Vokhshoori & McCarthy, 2014). Isoscapes of δ^{15}N are useful for assessing spatial patterns in fundamental N cycle processes, such as the influence of N_2 fixation, denitrification, and anthropogenic nutrients as shown in Figure 5 (e.g., Graham *et al.* , 2010; Vokhshoori & McCarthy, 2014; Schell *et al.* , 1998). Creating detailed and accurate isoscapes can ultimately help us better understand coastal marine ecosystems by providing a link between biogeochemical processes and food-web structures.

Isoscapes are invaluable tools used to better our understanding of coastal processes, however, there are important considerations to address when assessing the informative potential of δ^{15}N isoscapes in organic matter. First, isoscapes provide

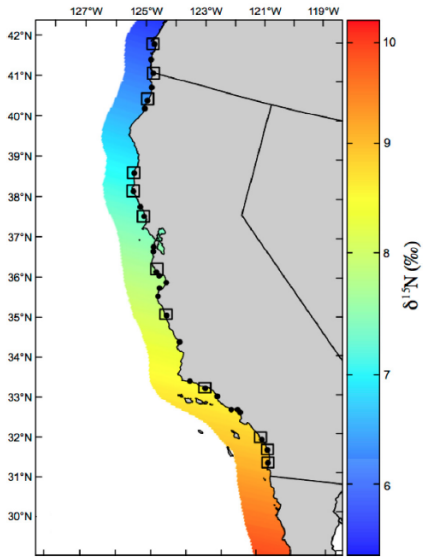

Figure 5: δ^{15}N Isoscape of the California Upwelling Current (Vokhshoori & McCarthy, 2014). This isoscape was created using δ^{15}N CSIA-AA on *M. californicus* specimen, which shows southward increase in δ^{15}N reflecting greater influence of denitrified waters originating from the Eastern Tropical North Pacific.

measured δ^{15}N values that are an estimate of "baseline" that is offset from the measured δ^{15}N of primary production when using secondary consumers or higher (e.g., Hobson *et al.* , 2012; Germain *et al.* , 2013). The inherent problem with this approach is that it does not account for the accumulation of ^{15}N with trophic transfer from each consumer in the food-chain. A canonical trophic enrichment factor of 3.4‰ is assumed in ecological studies (DeNiro & Epstein, 1978; Post, 2002), however, it has been proven that this average is highly variable between species (Post, 2002; McCutchan Jr *et al.* , 2003). Therefore it becomes difficult to accurately interpret baseline δ^{15}N values. Alternatively, primary producers such as seaweeds and seagrasses are sometimes used to map spatial variability baseline δ^{15}N (McIver *et al.* , 2018; Howarth *et al.* , 2019). However, the short-lived nature of these organisms means that they are influenced by short-term variability in N-cycle dynamics.

1.2.8 Mussels: The ideal bioindicator

The Blue mussel (*Mytilus edulis*) is a sessile organism found along the littoral zone of Nova Scotia. Mussels are an ideal "baseline indicator" organism because they continuously filter particulate organic matter (POM), integrating POM into their tissues for periods of 3-4 months (Hawkins *et al.* , 1986). As such, mussels provide a robust representation of long term biogeochemical patterns of nutrient inputs in the coastal zone. Within NS, studies have shown that *M. edulis* can filter approximately 5-20% of the volume of the inner basins of Ship Harbour per day, suggesting that mussels are ideal bioindicators for measuring the detectable impact of ambient levels of nutrients within the coastal zone (Strain, 2002). Because of their sessile nature, accessible coastal distribution, and continuous integration of POM, mussels are the ideal bioindicator to characterize Nova Scotia's baseline coastal δ^{15}N isoscape.

1.3 Previous Work

The following summarizes a few of the key studies on coastal eutrophication and δ^{15}N in Nova Scotia. Strain & Yeats (1999) evaluated chemical measurements as potential predictors of eutrophication within 34 sites in inlets on the Nova Scotia coast. Nutrient concentrations (silicate, phosphate, nitrate, nitrite, ammonia), dissolved oxygen, and trace metals like iron and manganese measurements were taken from samples collected in early autumn, when eutrophication is expected to be the most severe. Strain & Yeats (1999) ranked these sites based on an apparent eutrophication factor between these nutrient concentration measurements. This allowed them to evaluate the influence of inlet geometry on the eutrophication status of these inlets. One of the key findings within this study is that the presence of a sill and the degree to which the sill interferes with water circulation from the inlet to the open ocean, are the dominant geometric factors that contribute to eutrophication in these Nova Scotia inlets. These semi-enclosed basins create restricted circulation and promote denitrification (Strain & Yeats, 1999). Ryan *et al.* (2008b) refined the

eutrophication factors to N and P measurements, and found that overall result is that most of the inlets in NS are not eutrophic, with the exception of Barrington Bay, New Harbour, and the LaHave River.

Nagel *et al.* (2018) conducted a study using a nitrogen loading model (NLM) to estimate the rates of nitrogen input from point and non-point sources in 21 bays across the province. The sites selected for this study were based on known locations of eelgrass *Zostera marina* habitats because they provide essential habitat and food for an array of migratory species, as well as providing important ecosystem services like sediment stabilization and carbon sequestration. The study found that atmospheric deposition was the primary source of N in Nova Scotia (contributing 73 % of the total nitrogen loading), followed by agricultural runoff (Nagel *et al.* , 2018). This study did not measure δ^{15}N values within the 21 sites assessed using the NLM, however, analogous work conducted in New Brunswick applied both δ^{15}N and NLM to seven bays to estimate the magnitude and sources of nitrogen loading within these inlets (McIver, 2015). The maximum watershed area found in Nova Scotia was comparable to the maximum estimates found in New Brunswick (Nagel *et al.* , 2018; McIver, 2015). The isotopes measured in New Brunswick reflected the distinction between the two major N sources (atomspheric and human waste), with high δ^{15}N of 8-10 ‰ related to domestic N sources (McIver, 2015).

A more targeted δ^{15}N approach used to understand anthropogenic nitrogen within Nova Scotia was conducted by Howarth *et al.* (2019). This study aimed to discover if macroalgae species could map the isotopic footprints of multiple effluents, specifically of sewage wastewater contamination and salmon aquaculture. Two species of macroalgae *(Chondrus crispus and Palmaria palmata)* were deployed in a bay surrounding the aquaculture pens and the local sewage treatment facility. The δ^{15}N values were measured in bulk tissue, which ranged from 1.70 $\pm$ 0.06 ‰ to 4.32 $\pm$ 0.03 ‰ (Howarth *et al.* , 2019). These δ^{15}N values are lower than the expected background for seawater nitrate ($\delta^{15}N_{NO3}$), which averages 5-6 ‰ for thermocline

waters offshore Nova Scotia (Sherwood *et al.* , 2011). Howarth *et al.* (2019) tested the validity of using macroalgae as bioindicators used to map more than one effluent source but this offset from expected $\delta^{15}N_{NO3}$ values may be attributed to the species selected for this study. Both macroalgal species exhibited elevated tissue N concentrations near each source but exhibited elemental compositions that varied in distance. *P. palmata* had also not shown $\delta^{15}N$ values that changed over the 10 day incubation period in the field. These results highlight that the use of macroalgae $\delta^{15}N$ as a nutrient bioindicator technique may not always be straightforward.

1.4 Thesis Objective: Purpose of the Study

This study builds on analogous work conducted along the California coastline (Vokhshoori & McCarthy, 2014), but provides a new contribution to the field of stable isotope ecology by being conducted in a region with few previously published N isotopic measurements. Bulk and compound-specific $\delta^{15}N$ analysis were used to understand and describe the spatial variability of nitrogen isotopes at the base of the marine foodweb to provide the initial representation of Nova Scotia's regional gradients in respect to N sources and sinks. The hypothesis of this study is that the regional background isoscape of coastal NS will be overprinted by localized processes, including nitrogen from anthropogenic sources such as urban and agricultural runoff, and naturally occurring nitrification within the semi-restricted basins.

This project has three primary objectives designed to test the validity of the hypothesis that the regional background isoscape of coastal NS will be overprinted by localized inputs of nitrogen:

1. Assess nutrient concentrations and ratios in water samples.
2. Map the spatial distribution of nitrogen stable isotopes ($\delta^{15}N$) at the base of the marine foodweb in coastal Nova Scotia in a region with few published N isotopic measurements;

3. Determine whether the use of Compound Specific Isotope Analysis of Amino Acids can be used as a proxy for the δ^{15}N of primary production within highly dynamic coastal regions;

2 Methods

2.1 Sample Collection and Preparation

Specimens of blue mussels (*Mytilus edulis*) were collected from sites across Nova Scotia (Figure 6) under the permission of the Department of Fisheries and Oceans Canada (DFO) permit. The site permit numbers were 353410,353432 for the Atlantic region and SG-RHQ-18-169 for the Gulf region.

Mussels were collected from September to November in autumn of 2018. Sites were chosen opportunistically to cover a broad distribution of the province's shoreline, with 61 sites visited along the Atlantic and Northumberland coasts. The goal was to sample sites from a wide range of geographic and environmental regions, which include samples taken from poorly mixed basins surrounded by urban centres, sites nearby salmon aquaculture pens, and headlands exposed to the open ocean. Of the 61 sites visited, water and mussel samples were collected from 21 locations across the province because mussels were not found at all locations. Sites were classified as "open" or "closed" based on the shellfish collection ban outlined by the online Canadian Shellfish Monitoring Program (CSSP 2016). Areas where the collection ban was implemented follow the recommendations of Environment Canada, based on sanitary and bacteriological water quality conditions of mussels and other shellfish. Specimens of *M. edulis* were collected in triplicate, wherever possible, and immediately placed on ice until returned to the lab for further preparation. The adductor muscle was then dissected from the rest of the tissues before freeze-drying, while the shells were air-dried. The shells, adductor muscle, and remaining tissues were weighed before and after freeze-drying.

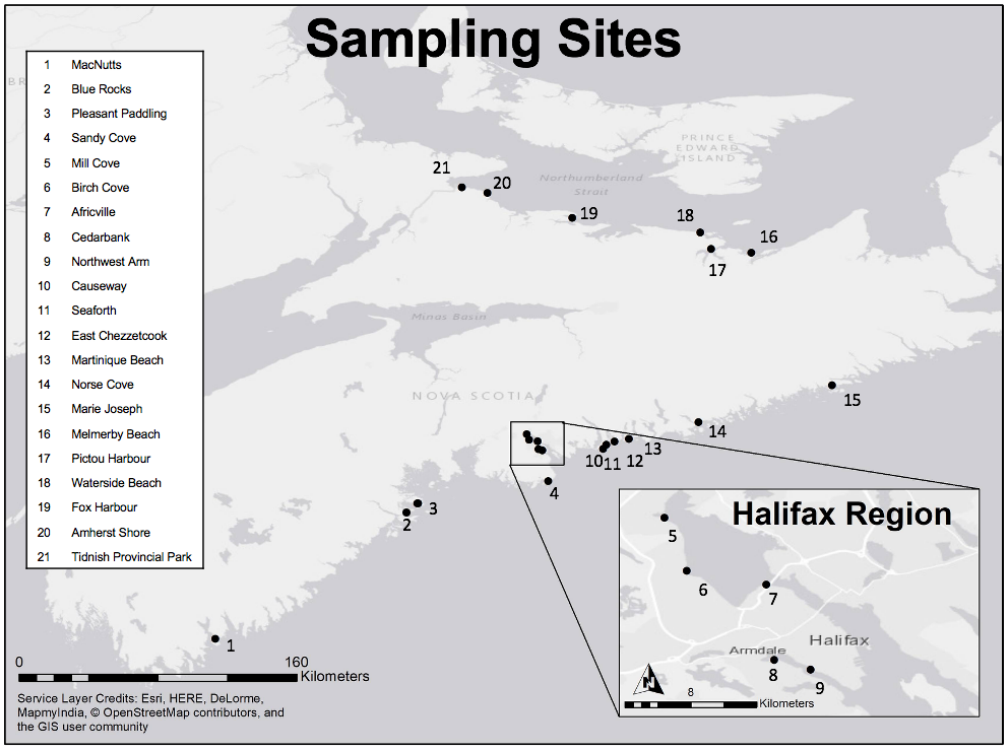

Figure 6: Sites across Nova Scotia where specimen of *M. edulis* and water samples were collected for this study.

2.2 Water Sample Analysis

Water samples were collected by wading into ∼0.5m water depth with a bucket, which was rinsed in triplicate before being returned to the shore. The sample collection bottles (0 mL Nalgene IP2 High density Polyethylene bottles) were rinsed three times with the water in the bucket. Using a 0.45 um Whatman disposable sterile syringe filter (25 mm diameter), the bottle was then rinsed once with filtered sample water to remove any particles that may have stuck to the sides of the bottles during the initial rinses. After the filtered rinse, the bottle was filled with 30 mL of filtered-water into the bottle. Samples were kept on ice until returned to the lab where they were stored in a -20°C freezer.

Nutrient concentrations of the water samples were analyzed in the Buchwald and CERC Ocean laboratories at Dalhousie University. Samples were analyzed for Nitrate (NO_3^-), Nitrite (NO_2^-), Ammonium (NH_4^+), and Phosphate (PO_4^{3-})

concentrations as described in Table 2. Ammonium and Phosphate concentrations were measured in the Buchwald Laboratory where Ammonium was measured in duplicate using a Thermo Scientific Evolution 260 Bio UV-Visible. Ammonium chloride samples were used as a standard and were measured at 0 uM, 1 uM, 2.5 uM, 5 uM, 10 uM, and 25 uM concentrations. Phosphate samples were run once using the Auto Analyzer AA3. Standards of Potassium dihydrogen phosphate were used at 0.2 uM, 0.5 uM, 0.8 uM, 1.5 uM, and 2 uM. All other nutrient concentrations (Nitrate and Nitrite) were measured in triplicate using a Skalar SAN++ Continuous Flow Nutrient Analyzer. Nitrate and Nitrite concentrations were measured in the CERC Ocean Laboratory following methodology established by Hydes *et al.* (2010) and protocol outlined in McGrath *et al.* (2019). Reference material for Nitrate and Nitrite, produced by Kanso Co. LTD (Aoyama *et al.* , 2010), were used for quality control. The analytical reproducibility associated with running triplicate samples of Nitrite was $<\pm 0.02‰$and $<\pm 0.15‰$for Nitrate.

Table 1: Instrumental level of detection (LOD) and quantification (LOQ) for water samples measured in the CERC Ocean Laboratory.

	Nitrate	Nitrite	Ammonium	Phosphate
LOD	0.05	0.01	0.06	0.01
LOQ	0.16	0.02	0.19	0.04

2.2.1 Nutrient Ratios: F-Ratio

Nutrient concentrations provide a limited representation of oceanographic patterns, however, nutrient *ratios* can be useful metrics used as indicators of fundamental nitrogen cycle processes (i.e. nitrification and denitrification). F-Ratio is used to asses nitrogenous supply to the photic zone through the classification of "new" versus "recycled" nitrogen sources (Dugdale & Goering, 1967). F-ratio typically measures the ambient uptake rates of Nitrate relative to Ammonium. For the purpose of this study, however, a pseudo f-ratio is presented using nutrient concentrations rather

than uptake rates. This relationship is defined by:

$$\frac{NO_3^-}{NO_3^- + NH_4} \tag{3}$$

where NO_3^- in the numerator is the nitrate concentration and the denominator, of nitrate plus ammonium (NH_4), is the regenerated and reduced-N (Eppley & Peterson, 1979). Nitrate represents "new nitrogen" because it is introduced to surface waters by the upwelling of deeper water where remineralization of organic nitrogen occurs. In contrast, ammonium represents "recycled nitrogen" because it is provided by the immediate breakdown of organic matter. Thus, higher f-ratios correspond with relatively more new nitrogen whereas lower values represent relatively more recycled nitrogen (Dugdale & Goering, 1967).

2.2.2 Nutrient Ratios: N* Index

Another important analysis of the nutrient concentrations is through the use of N* as a tracer of denitrification and N_2 fixation. N* is the linear combination of nitrate and phosphate defined as:

$$N^* = NO_3 - 16 \cdot PO_4 + 2.9 \tag{4}$$

where -16 accounts for the Redfield stoichiometric N:P ratio of 1:16 and 2.9 µmol/kg was added to bring the global mean N* to zero (Gruber & Sarmiento, 1997). This means that N* is an index of nitrogen being added (via N_2 fixation) or removed (via denitrification) from the ocean, based on deviation of the Redfield ratio. Figure 7 demonstrates the relationship between N_2 fixation, denitrification and N*.

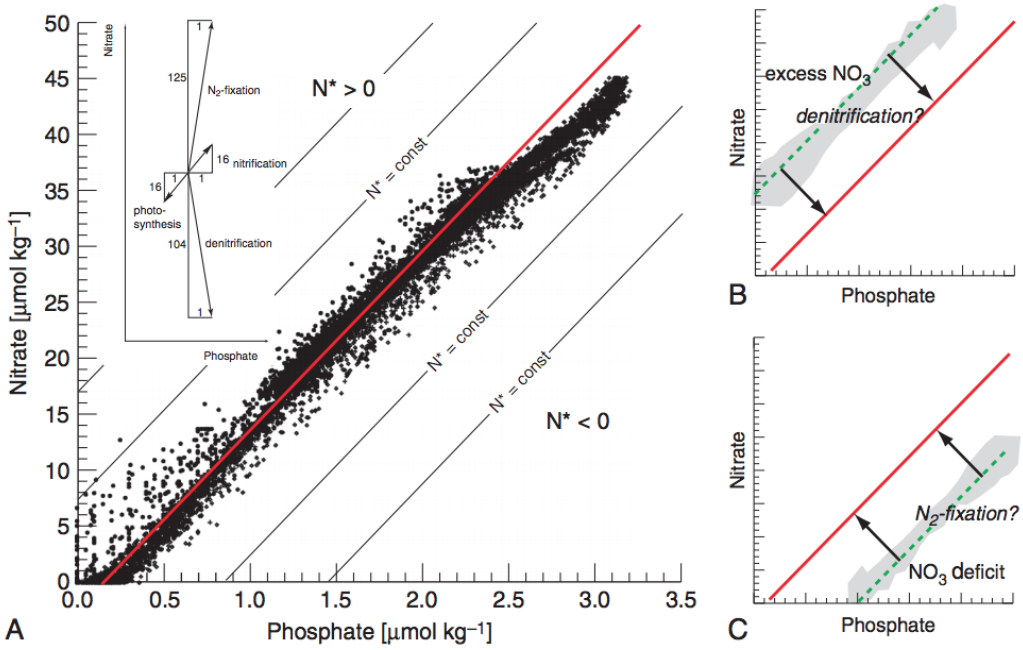

Figure 7: (A) Plot of NO_3^- versus PO_4^{3-} from all depths and ocean basins selected from WOCE cruises. The inset shows how various biogeochemical processes influence NO_3^- and PO_4^{3-} distribution. The red line shows the constant Redfield ratio, with a slope of 16:1. The black lines show N* trends. (B) and (C) show hypothetical distributions of what happens to N* when NO_3^- is in excess and deficit, respectively (Gruber, 2004)

2.3 Mussel Physiology

Bivalve condition index (CI) is a parameter that can be used to assess mussel physiology (Filgueira *et al.* , 2013). This index is quantified by:

$$\text{Bivalve Condition Index} = \frac{\text{Dry Meat Weight}}{\text{Dry Shell Weight}} \times 100. \tag{5}$$

CI does not account for potential variations in internal cavity capacity (Mann, 1978) and therefore nutritive status (Crosby, 1990). This means that it serves as a rough estimate of mussel physiology, but is widely used because it is easily standardized and suitable for universal applications as opposed to other indices.

2.4 Bulk Stable δ^{15}N Nitrogen Analysis

Stable nitrogen analysis ($\delta^{15}N_{bulk}$ and $\delta^{13}C_{bulk}$) was conducted in the CERC Ocean Laboratory at Dalhousie University. *M. edulis* adductor tissues were homog-

enized with mortar and pestle. Aliquots of approximately 0.15mg were packed in tin capsules before being combusted in a Vario Micro Cube at 1150°C. This flash combustion reduces nitrogen and carbon compounds within the sample to N_2 and CO_2 products, respectively. The N_2 gas was separated from any CO_2 products with a temperature programmed desorption trap. The gaseous nitrogen components were then carried by ultrapure helium to the Isoprime 100 continuous flow isotope ratio mass spectrometer (EA-IRMS) for δ^{15}N and δ^{13}C analysis. Analytical error, based on analysis of sample duplicates, was typically $<\pm 0.3‰$. Standard deviations of average δ^{15}N bulk values were used to gauge intra-site variability among sample locations.

2.5 Compound-Specific δ^{15}N Isotope Analysis of Amino Acids

To refine baseline δ^{15}N estimates independent of trophic fractionation, 8 sites were chosen for compound-specific isotope analysis based on bulk δ^{15}N results. Compound-specific isotope analysis was conducted in the Stable Isotope Biogeochemistry Lab (SIBL) at Dalhousie University. Amino acid δ^{15}N values were obtained through a process of hydrolysis, cation exchange, isopropyl TFAA derivatization, and Gas Chromatograph - Isotope Ratio Mass Spectrometer (GC-IRMS) analysis after previously published procedures by Silfer *et al.* (1991) and McCarthy *et al.* (2007).

2.5.1 Hydrolysis

AAs in organic material, such as muscle tissues, exist in a "bound" form within the peptide bonds of proteins (Ohkouchi *et al.* , 2017). Hydrolysis is the initial procedure in the CSIA-AA methodology, which breaks the peptide bonds of the constituent proteins that house the AAs. A mass of 5mg of the dried and homogenized adductor muscle was added to a 9ml borosilicate glass tube. A volume of 2 ml of 6N HCl was added to the tube. The tube was then flushed with N_2 gas for 10 seconds to remove oxygen, and then quickly capped. The tube was then heated

at 110°C for 20 hours. These sample hydrolysates were dried down under a gentle stream of N_2 gas, then immediately resuspended in 0.01N HCl, and stored at 4°C until further processing.

2.5.2 Cation Exchange Chromatography

The hydrolysis process produces many molecules besides the desired free AAs that should be extracted before derivitization. Cation-exchange chromatography is used to remove these interfering lipids and other materials from the organic sample. Sample hydrolysates were transferred to pasteur pipettes, packed with Dowex WX-8 resin and then eluted using 4 x 1 mL rinses of 2 N ammonium hydroxide to separate the lipids from the AAs. The samples were then dried-down using N_2 gas before being re-hydrolyzed, heated at 110°C for 5 minutes, and cooled to room temperature in preparation for derivatization.

2.5.3 Derivatization

AAs must be derivatized to reduce polarity and increase volatility so that they can be analysed on a GC-IRMS. The basic chemical reaction is shown in Figure 8. The polar carboyxl (-COOH), amine (-NH_2), and hydroxyl (-OH) groups of AAs are neutralized during the derivatization process by replacing the hydrogen atoms with nonpolar moieties. To make the AAs more volatile, a modified version of the derivatization protocols described by Silfer *et al.* (1991) was used. Briefly, samples were esterified by heating in a mixture of acidified 2-Propanol (1:5 of 1 mL Acetyl Chloride for every 5 mL of 2-Propanol) at 110°C for 1 hour. Samples were then acylated by heating in a 1:3 mixture of Dichloromethane: Trifluroacetyl acetate (DCM: TFAA) at 100°C for 15 minutes.

Samples were further purified using a solvent extraction method adapted from Popp *et al.* (2007). Samples were dried under N_2 gas for 30 minutes, then resuspended in a mixture of 2 mL of Chloroform and 2 mL of "P-buffer" solution (1 M potassium phosphate: 1 M sodium phosphate). After centrifuging at 3000 rpm

for 5 minutes, the chloroform layer containing the AAs was pipetted into a new borosilicate glass vial. The chloroform was then evaporated under N_2 gas and the acylation step (2.5.3) was repeated. In preparation for gas chromatography, 1 mL of each organic sample was suspended in 0.5-1.0 mL of Ethyl Acetate before being analysed for δ^{15}N content of each amino acid.

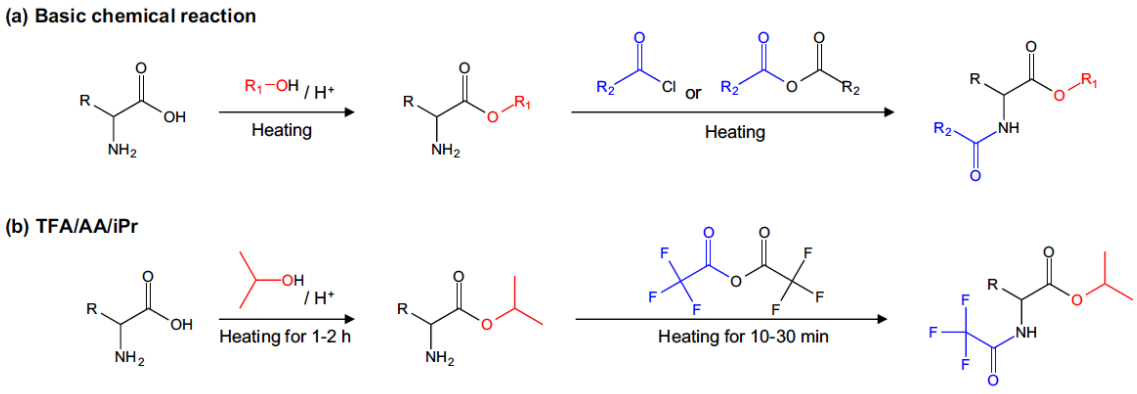

Figure 8: Amino acid derivatization process, adapted from Ohkouchi *et al.* (2017). Diagrams show: (a) Basic chemical AA derivatization reaction, (b) AA chemical reaction when using trifluoroacyl-isopropyl esters (TFA/AA/iPr).

2.5.4 GC-IRMS

Amino acid δ^{15}N values were obtained through a Thermo Trace 1310 Gas Chromatograph, coupled via GC Isolink II and Conflo IV universal interface to a Delta V Plus Isotope Ratio Mass Spectrometer. Samples were injected in triplicate and bracketed by standards so that δ^{15}N results could be corrected based on the known average standard values through each run. In addition, we used Norleucine (Nle) as an internal standard in each sample because the δ^{15}N value has been independently determined. Instrumental precision varied for individual AAs but was typically $<\pm 1.0‰$.

Under our analytical conditions, δ^{15}N values were obtained for Alanine (Ala), Aspartic Acid (Asp), Glutamic Acid (Glu), Isoleucine (Ile), Leucine (Leu), Proline (Pro), Valine (Val), Glycine (Gly), Phenylalanine (Phe), Lysine (Lys), Threonine

(Thr), and Serine (Ser). Sample reproducibility averaged $\lesssim 1‰$ among individual AAs.

2.6 Amino Acid Groupings and Trophic Position Estimates

Amino acids were categorized into four main designations: "Trophic", "Source" (*after* Popp *et al.* 2007), "Metabolic" which exclusively defines Thr (*after* Germain *et al.* 2013) and "Intermediate." The Trophic AAs heavily fractionate with each trophic step and are represented by Glu, Asp, Ala, Leu, Ile, Pro, and Val. The Source AAs (little expcted change to ^{15}N at higher trophic levels) comprise Phe and Lys. The Intermediate AAs will refer to Gly and Ser, which have poorly understood ^{15}N behaviour with regard to metabolic fractionation (Germain *et al.* , 2013).

Based on this framework, average Trophic and Source δ^{15}N values were calculated:

$$Trophic\,AA\,\delta^{15}N = Average\,\delta^{15}N[Glu, Asp, Ala, Leu, Ile, Pro, Val] \tag{6}$$

$$Source\,AA\,\delta^{15}N = Average\,\delta^{15}N[Phe, Lys] \tag{7}$$

2.7 Mole Percent Calculations and Weighted Averages

Amino acid molar concentrations were calculated for the 8 sites selected for CSIA-AA. The equation is defined as:

$$Mole\,Percent\delta^{15}N = \frac{Individual\,AA\,Molar\,Amount}{\sum All\,AA\,Molar\,Amounts} \tag{8}$$

where the individual AA molar amount is calibrated using internal standards that bracket the injections. The slope of the standard's average peak area was multiplied by the sample's average peak area to produce the molar amount for each AA. These individual AA molar amounts are summed, as expressed in the denominator.

Once the mole percent was calculated for each individual AA in every sample, it became possible to determine the weighted average δ^{15}N of these samples. This was done using the following equation:

$$Weighted\ Average\ \delta^{15}N = \frac{Mole\ Percent \times \delta^{15}N_{AA}}{100} \tag{9}$$

where the mole percent was multiplied by the measured $\delta^{15}N_{AA}$ value of each individual AA within the sample, before being divided by the sum total, 100.

2.8 Trophic Position Estimates

Trophic position calculations were calculated using the canonical Trophic and Source AAs (Glu and Phe, respectively) in the following equation defined by Chikaraishi *et al.* (2009):

$$TP_{Glu-Phe} = \frac{(\delta^{15}N_{Glu} - \delta^{15}N_{Phe}) - 3.4}{7.6} + 1 \tag{10}$$

Where δ ^{15}N$_{Glu}$ - δ ^{15}N$_{Phe}$ are measured values, 3.4 is the assumed isotopic difference between Glu and Phe in primary producers, often referred to as β (Chikaraishi *et al.* , 2009). The value of 7.6 is the assumed ^{15}N enrichment in Glu relative to Phe with each trophic transfer from food source to consumer, often called the Δ value (Chikaraishi *et al.* , 2009).

2.9 Microbial Resynthesis Index

The $\sum V$ parameter is a proxy for total heterotrophic resynthesis, based on average deviation in δ^{15}N of the Trophic AAs. This relationship is defined as:

$$\sum V = \frac{1}{n} \sum Abs(x_{AA}) \tag{11}$$

where x is the deviation of each Trophic AA=[δ ^{15}N$_{AA}$ $-$ AVG δ ^{15}N(Glu, Asp,

Ala, Leu, Ile, Pro, Val)], and n=the total number of Trophic AAs used in the calculation.

2.10 Statistical Analysis and Calculations

Tests run for this project focused on N variability within water samples and the adductor muscle of *M. edulis* specimens. Mean and standard deviations were compared for all parameters, but it was not possible to identify patterns among these variables without the use of robust statistical tests. Welch Two Sample T-Tests were used to assess the correlation between $\delta^{15}N_{Bulk}$ versus region and habitat type, as shown in Table 3 (Yuen, 1974). Linear regression models were conducted on $\delta^{15}N_{Bulk}$ versus F-ratio and N* to evaluate the significance of using nutrient ratios as indices for N isotopic behaviour within the water samples (Table 4). Finally, principle component analysis (PCA) was used to reduce the dimensionality of the dataset. The variables of the PCA conducted in this study were $\delta^{15}N_{Phe}$, $\delta^{13}C$, TP, and $\sum V$ (Figure 19). All statistical tests were conducted using RStudio software.

3 Results

3.1 Nutrient Data

Water samples were collected from 21 sites across Nova Scotia during autumn of 2018 (September to November), as shown in Figure 6. Samples were measured for nitrite, nitrate, ammonium, and phosphate concentrations, as outlined in Table 2. Nitrite values ranged from 0.03µM to 0.26 µM, with an average concentration of 0.18 ± 0.08 µM; n=21. Nitrate ranged from 0.07 µM to 15.19 µM and averaged 5.23 ± 4.94 µM; n=21. Ammonium concentrations shared similar variability, with an average concentration of 1.33 ± 1.09 µM. The range of ammonium values was 0.133 µM to 4.796 µM. Phosphate ranged from 0.21 to 1.05µM. The average phosphate value was 0.55 ± 0.26µM; n=21. The highest nitrite and phosphate concentrations (0.27 ± 0.08 µM and 1.05 ± 0.26µM, respectively) were found at Cedarbank, while Mill Cove had the highest nitrate (15.19 ± 4.94 µM) and ammonium (4.80 ± 1.09 µM) concentrations.

Water samples collected from Martinique, Blue Rocks, Waterside Beach South, Marie Joseph, Fox Harbour, Pictou Harbour, Causeway Road, and Tidnish Provincial Park had nitrite values that were below level of detection (<0.01). Norse Cove, East Chezzetcook and Seaforth also had nitrite values under the level of quantification (<0.02). These non-detect samples were given a value of 0µM when calculaing the average concentrations listed above. Nitrate was the only other nutrient with samples below the level of quantification (<0.16). These were located at Martinique, Blue Rocks, Waterside Beach South, Marie Joseph, Fox Harbour, Pictou Harbour, and Norse Cove.

Table 2: Nutrient Concentrations and Ratios Data Table. Values are expressed in units of µM. Nitrite, nitrate and phosphate were measured in triplicate, with standard deviations listed in brackets. Only one measurement was conducted for Ammonium. Nutrient concentrations and N* are expressed in µM kg^{-1}; F-ratio and N:P are unitless.

Site	NO_2^-	NO_3^-	PO_4^{3-}	NH_4^+	F-ratio	N:P	N*
Africville	0.16 (0.00)	10.27 (0.04)	1.04 (0.01)	3.37	0.75	13.31	-3.42
Amherst Shore	0.26 (0.01)	13.16 (0.15)	0.92 (0.03)	1.53	0.90	16.19	1.29
Birch Cove	0.15 (0.00)	10.21 (0.03)	1.05 (0.01)	1.36	0.88	11.16	-3.69
Blue Rocks	0.01 (0.02)	0.10 (0.01)	0.29 (0.01)	0.13	0.42	0.83	-1.7
Causeway Rd	0.01 (0.00)	0.17 (0.02)	0.26 (0.00)	0.54	0.24	2.77	-1.09
Cedar Bank	0.27 (0.01)	7.68 (0.06)	0.66 (0.00)	2.38	0.76	15.64	0.02
East Chezzetcook	0.02 (0.01)	0.18 (0.00)	0.37 (0.00)	1.61	0.1	4.9	-2.84
Fox Harbour	0.00 (0.00)	0.13 (0.01)	0.21 (0.01)	0.33	N/A	N/A	N/A
MacNutts	0.23 (0.02)	2.79 (0.03)	0.35 (0.00)	1.12	0.71	11.84	0.09
Marie Joseph	0.01 (0.01)	0.11 (0.02)	0.42 (0.00)	2.08	N/A	N/A	N/A
Martinique	0.00 (0.01)	0.07 (0.02)	0.42 (0.01)	0.93	N/A	N/A	N/A
Melmerby Beach	0.11 (0.01)	1.91 (0.04)	0.55 (0.01)	2.43	0.44	8.14	-3.93
Mill Cove	0.18 (0.00)	15.19 (0.03)	0.97 (0.02)	4.80	0.76	20.86	2.63
Norse Cove	0.02 (0.00)	0.15 (0.02)	0.61 (0.01)	1.18	N/A	N/A	N/A
Northwest Arm	0.26 (0.01)	5.16 (0.02)	0.68 (0.01)	1.22	0.05	3.1	-3.7
Pictou Harbour	0.00 (0.00)	0.15 (0.02)	0.60 (0.01)	0.58	N/A	N/A	N/A
Pleasant Paddling	0.03 (0.01)	1.9 (0.06)	0.36 (0.01)	0.80	0.70	7.53	-1.01
Sandy Cove	0.12 (0.01)	1.87 (0.03)	0.50 (0.01)	0.38	0.83	4.78	-3.17
Seaforth	0.02 (0.01)	2.58 (0.02)	0.30 (0.00)	0.61	0.81	10.69	0.68
Tidnish	0.00 (0.01)	0.17 (0.01)	0.35 (0.01)	0.42	0.29	1.68	-2.48
Waterside Beach	0.00 (0.00)	0.13 (0.01)	0.70 (0.01)	0.54	N/A	N/A	N/A

3.1.1 Nutrient Ratios: F-Ratio

Nutrient ratios can provide a more comprehensive representation of fundamental nitrogen cycle processes than nutrient concentrations. F-Ratio is a useful metric used to classify "new" versus "recycled" nitrogen sources (Dugdale & Goering, 1967). F-ratios calculated using Equation 3 ranged from 0.10 to 0.90, with an average f-ratio of 0.61 ± 0.26; n=16 (Table 2). Figure 9 shows the relationship between f-ratio and nitrate concentration within the 21 water samples. Samples collected from Martinique, Blue Rocks, Waterside Beach, Marie Joseph, Fox Harbour, Pictou Harbour, and Norse Cove had nitrate values below the limit of quantification (<0.16). F-ratios calculated for these sample sites were omitted from the reported range and average values but can be found in Figure 9 and Table 2. East Chezzetcook had the lowest f-ratio values at 0.10 ± 0.26 while samples collected from Amherst Shore were the highest at 0.90 ± 0.26.

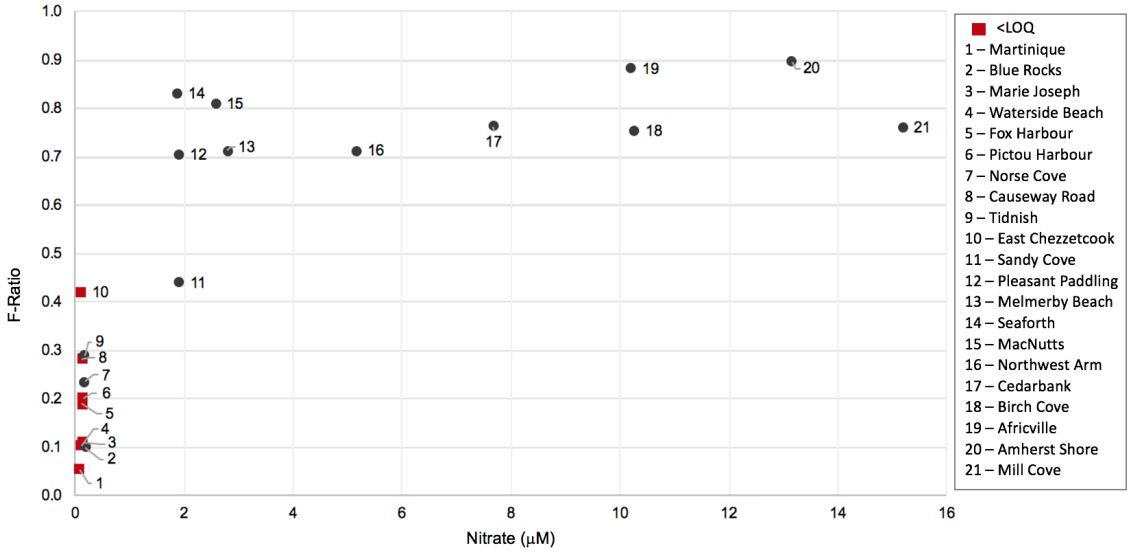

Figure 9: Calculated F-ratio values from 21 water samples at sites in Nova Scotia. The red squares are sites below the level of quantification (<LOQ) of Nitrate (<0.16). These sites are Martinique, Blue Rocks, Waterside Beach, Marie Joseph, Fox Harbour, Pictou Harbour, and Norse Cove.

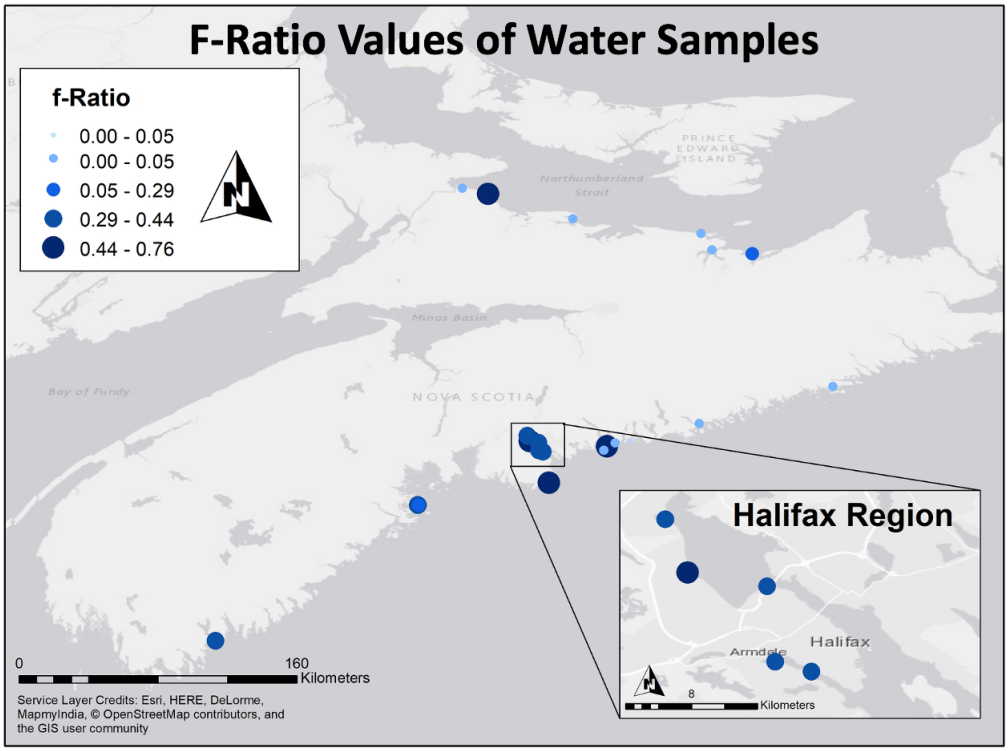

Figure 10: Spatial distribution map of calculated F-ratio values from 21 water samples at sites in Nova Scotia. Samples from Martinique, Blue Rocks, Waterside Beach, Marie Joseph, Fox Harbour, Pictou Harbour, and Norse Cove were below the level of quantification of nitrate (<0.16).

3.1.2 Nutrient Ratios: N* Index

Another important analysis of the nutrient concentrations is through the use of N* as a tracer of denitrification and N_2 fixation. N* values calculated using Equation 4 ranged from -3.93 to 2.63(n=14), with an average N* of -1.41. Samples from Martinique, Blue Rocks, Waterside Beach, Marie Joseph, Fox Harbour, Pictou Harbour, and Norse Cove fell below the level of quantification for nitrate (<0.16) and were therefore omitted (Table 2). Figure 11 shows a graph of NO_3^- versus PO_4^{3-} where all samples fall below the N:P (1:16) ratio.

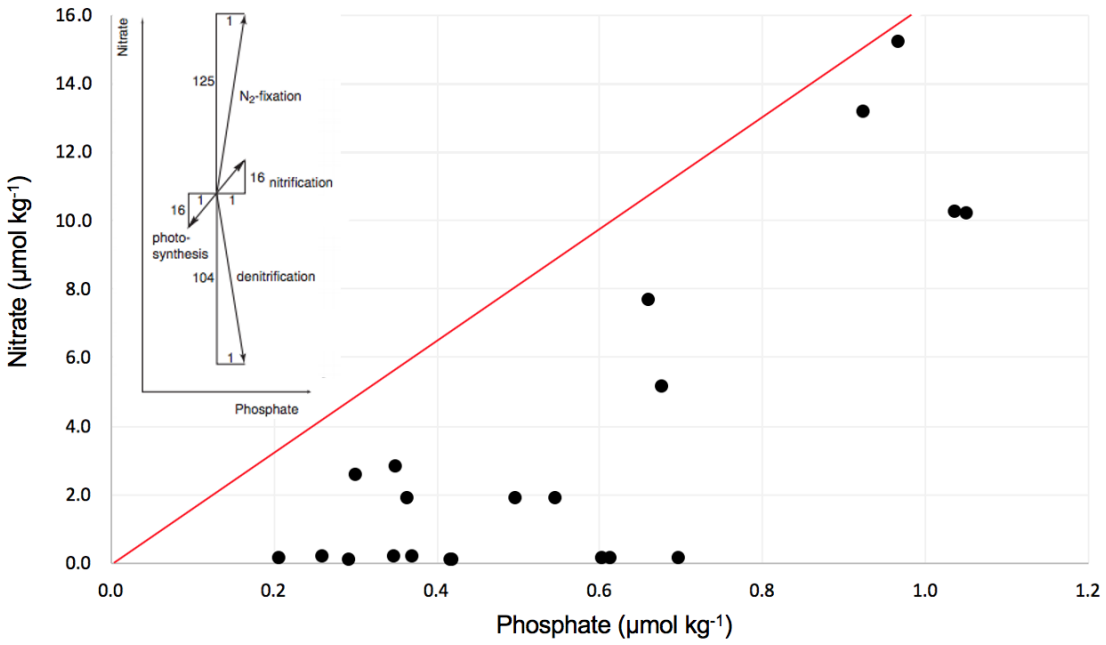

Figure 11: Plot of NO_3^- versus PO_4^{3-} from 21 water samples at sites in Nova Scotia (black circles). The inset shows how various biogeochemical processes influence NO_3^- and PO_4^{3-} distribution, adapted from Gruber (2004). The red line shows the constant Redfield ratio, with a slope of 16:1.

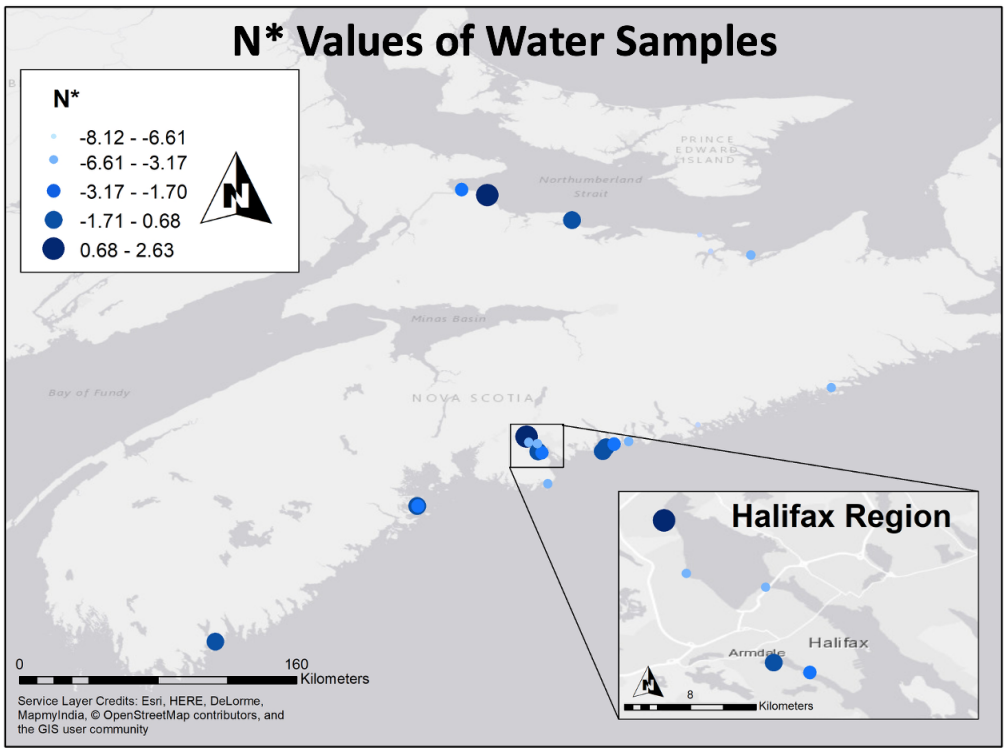

Figure 12: Map of Calculated N* Values.

3.2 Bulk Isotope Analysis

Bulk δ^{15}N and δ^{13}C isotope analysis was conducted on the adductor muscle of *M. edulis* specimen from 21 sites across Nova Scotia (Table **??**). Site averages bulk δ^{15}N ranged from 6.80 ± 0.27‰ to 11.08 ± 1.00‰; n=61. The average bulk δ^{15}N of all individual mussel samples was 8.99 ± 0.44‰; n=61. Site averages with noticeably low δ^{15}N bulk include Melmerby Beach (7.13 ± 0.27‰; n=4), MacNutts (7.82 ± 0.41‰; n=4) and Mill Cove (7.82 ± 0.59‰; n=4). In contrast, sites with the highest δ^{15}N bulk values include Cedar Bank (10.78‰; n=1) Pictou Harbour (10.20 ± 0.25‰; n=3) and Causeway Road (10.10 ± 0.29‰; n=3). Individual bulk δ^{13}C values ranged from -21.71 ± 0.23‰ to -14.78 ± 1.22‰; n=61. The average bulk δ^{13}C of individual *M. edulis* specimen was -18.73 ± 0.32‰; n=61. Amherst (-21.45 ± 0.23‰; n=4), MacNutts (-20.32 ± 0.23‰; n=4), and Tidnish (-20.71 ± 0.10‰; n=3) were among the lowest bulk δ^{13}C site averages. The site with the highest δ^{13}C site average was Melmerby Beach (-16.04 ± 1.22‰; n=4). Figure 13 shows the relationship between δ^{15}N and δ^{13}C. The P-Value for the linear regression describing this relationship is 0.088; n=61, therefore the result is not significant at $P<0.05$.

Figure 14 describes the relationship between bulk δ^{15}N and δ^{13}C isotope analysis and mussel physiology. Bivalve condition index (CI) was calculated using equation 5. CI site averages ranged from 9.60 to 83.22; n=21, with the average CI among sites being 38.11 ± 21.29; n=21. The relationship between both δ^{15}N and δ^{13}C versus CI were not significant linear regressions (P=0.35;n=21 and P=0.63, respectively). Samples collected from Africville had the most variation among individual samples collected from the same site, with CI calculated values of 5.38, 16.32, and 46.56 (average=22.75). At three sites, only one specimen was collected and it is therefore difficult to asses representativeness. These sites include Cedarbank (29.91), Norse Cove (55.61), Pleasant Paddling (13.87). By omitting these sites average CI becomes 36.84 ± 20.79; n=17. When omitting these CI values from the δ^{15}N (P=0.24;n=17)

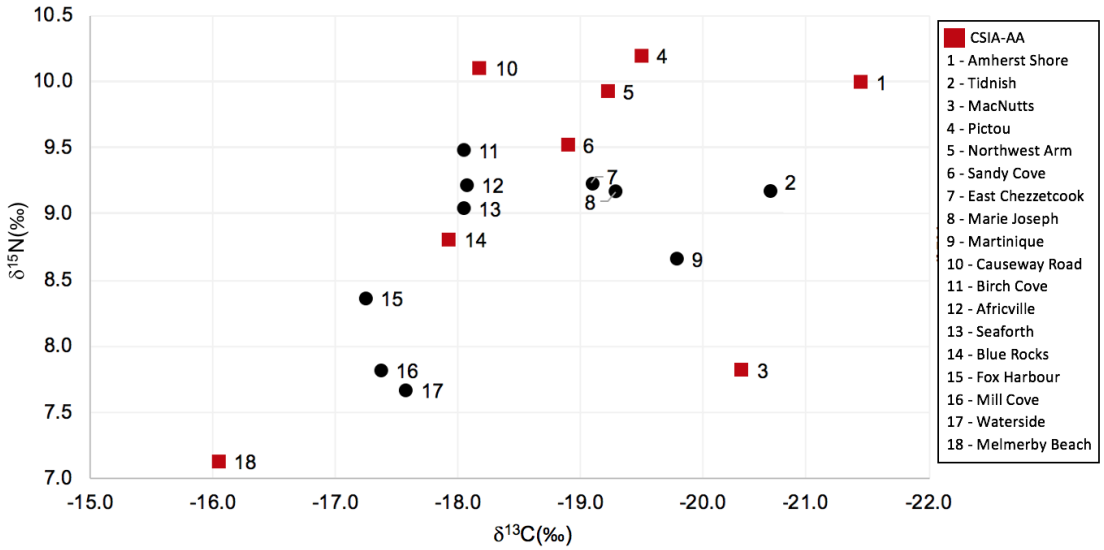

Figure 13: Relationship between measured bulk δ^{15}N and δ^{13}C for 18 sites where triplicate samples of *M. edulis* specimen were collected. This graph was used to select 8 sites for CSIA-AA, to show representative low, intermediate and high bulk values. These sites are: Amherst Shore, MacNutts, Pictou, Northwest Arm, Sandy Cove, Causeway Road, Blue Rocks, and Melmerby Beach.

and δ^{13}C (P=0.98;n=17) vs CI regressions, the relationships remain insignificant at the P<0.05 level.

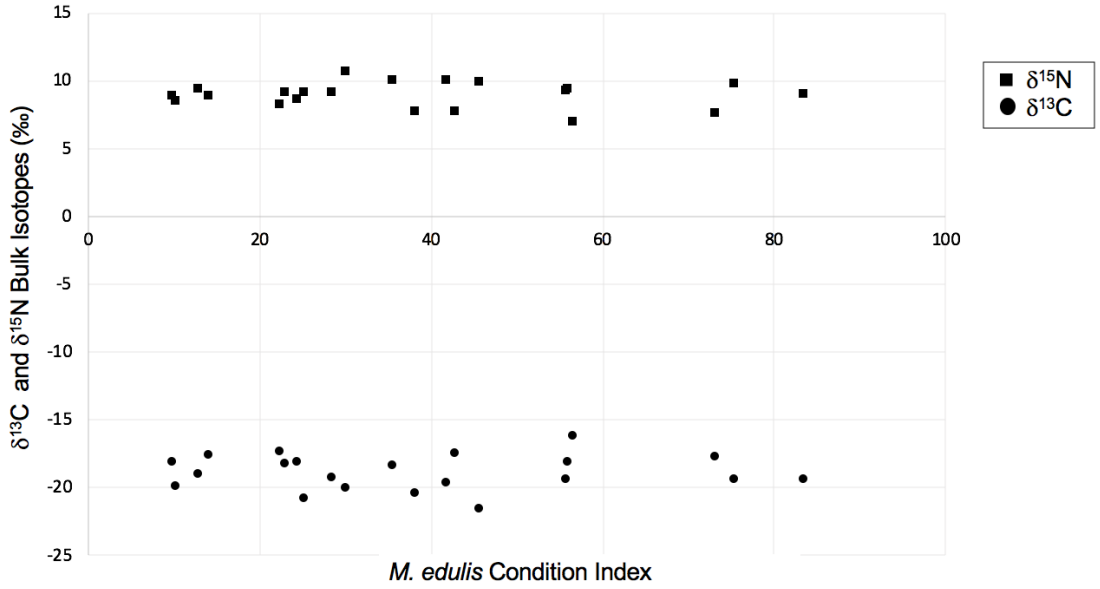

Figure 14: Bulk δ^{15}N and δ^{13}C versus calculated Bivalve Condition Index values, averaged by site.

Bulk δ^{15}N values were tested for the statistical relationships between region, habitat type, f-ratio, and N*. Welch Two Sample T-Tests were conducted on the coastline (Atlantic vs. Northumberland) and habitat type (estuarine vs. open ocean) to asses for differences with bulk δ^{15}N (Table 3). There was no significant difference (<P=0.05) for region (P=0.96) or habitat type (P=0.38). There was, however, a significant difference in site average $\delta^{15}N_{bulk}$ between sites without a collection ban (mean δ^{15}N = 8.51 ± 0.7 ‰, n = 10) and with a collection ban (mean δ^{15}N = 9.47 ± 0.7 ‰, n = 7) and between bulk δ^{15}N and the collection ban (P=0.016). Linear regressions conducted on F-ratio (P=0.93) and N* (0.86) showed no correlation with bulk δ^{15}N (Table 4).

Table 3: Bulk δ^{15}N vs Environmental Variables T-Test Values

Variable	T-Value	Degrees of Freedom	P-Value
Region	0.05	5	0.96
Habitat Type	0.90	15	0.38
Collection Ban	-2.67	15	0.016

Table 4: Linear Regressions of Bulk δ^{15}N vs Nutrient Ratios

Variable	Adjusted R^2	Degrees of Freedom	P-Value
F-Ratio	-0.06	16	0.93
N*	-0.06	16	0.86

Table 5: Collection sites and bulk δ^{15}N and δ^{13}C from *M. edulis* specimen.

Location	n	Latitude	Longitude	Shoreline	Habitat Type	Ban	δ^{13}C	δ^{15}N
Africville	3	44.6759	-63.6154	Atlantic	Estuarine	Yes	-18.06(0.8)	9.22(0.3)
Amherst Shore	3	45.9662	-63.8752	Northumberland	Open Ocean	N/A	-21.45(0.2)	10.0(0.1)
Birch Cove	3	44.6834	-63.6588	Atlantic	Estuarine	Yes	-18.04(0.2)	9.48(0.1)
Blue Rocks	3	44.3539	-64.2346	Atlantic	Open Ocean	No	-17.92(0.2)	8.81(0.1)
Causeway Rd	3	44.6369	-63.2745	Atlantic	Open Ocean	Yes	-18.18(0.2)	10.1(0.3)
Cedar Bank	1	44.6346	-63.6110	Atlantic	Estuarine	Yes	-19.84(0.0)	10.78(0.0)
East Chezzetcook	3	44.6754	-63.2155	Atlantic	Estuarine	No	-19.09(0.4)	9.23(0.2)
Fox Harbour	2	45.8362	-63.4343	Northumberland	Estuarine	No	-17.24(0.4)	8.37(0.0)
MacNutts	3	43.6506	-65.2867	Atlantic	Open Ocean	No	-20.32(0.2)	7.82(0.4)
Marie Joseph	3	44.9676	-62.0874	Atlantic	Estuarine	No	-19.28(0.2)	9.17(0.5)
Martinique	3	44.6888	-63.1417	Atlantic	Open Ocean	No	-19.78(0.3)	8.66(0.4)
Melmerby Beach	3	45.6550	-62.5054	Northumberland	Estuarine	No	-16.04(1.2)	7.13(0.3)
Mill Cove	3	44.7124	-63.6711	Atlantic	Estuarine	Yes	-17.37(0.4)	7.82(0.6)
Norse Cove	1	44.7757	-62.7799	Atlantic	Estuarine	Yes	-19.26(0.0)	9.43(0.0)
Northwest Arm	3	44.6294	-63.5911	Atlantic	Estuarine	Yes	-19.22(0.4)	9.93(1.0)
Pictou	3	45.6755	-62.7151	Northumberland	Estuarine	Yes	-19.49(0.1)	10.20(0.3)
Pleasant Paddling	1	44.3529	-64.2393	Atlantic	Estuarine	No	-17.47(0.0)	9.06(0.0)
Sandy Cove	3	44.4697	-63.5595	Atlantic	Open Ocean	Yes	-18.89(0.2)	9.52(0.2)
Seaforth	3	44.6586	-63.2581	Atlantic	Open Ocean	No	-18.04(0.2)	9.04(0.2)
Tidnish	3	45.9960	-64.0077	Northumberland	Open Ocean	No	-20.71(0.1)	9.24(0.3)
Waterside Beach	2	45.7595	-62.7710	Atlantic	Estuarine	No	-17.57(0.2)	7.67(0.0)

3.3 CSI-AA

3.3.1 Amino Acid Mole Percent Composition

During compound-specific isotope analysis, amino acid mole percent composition was measured. This was done on 22 samples from 8 of the 21 sites. Individual AAs measured were Alanine, Glycine, Threonine, Valine, Leucine, Isoleucine, Proline, Aspartic Acid, Glutamic Acid, Phenylalanine, and Lysine. These values were calculated using Equation 8 and ranged from 1.80 to 26.23 mol % (Figure 15). Serine, Tyrosine and Methionine peaks were too low to be quantified with the GC-IRMS. Histidine and Arginine were destroyed during the hydrolysis process and consequently were unable to be measured as well.

Glutamic Acid accounts for the majority of the AAs within the adductor muscle. In contrast, Phenylalanine, Proline, Valine, and Isoleucine were the least abundant. There is remarkable similarity to published samples Wilbur & Yonge (2013), following the trends of the AA mole percent composition of the *M. edulis*derived AAs in this study.

Coefficients of variation (CV) were calculated for the average value of individual AAs to assess the variability between each AA mole percent composition. Values ranged from 0.26 to 8.18; n=61. Aspartic acid had the lowest CV value of 0.26 and Threonine had the highest (8.18). The average CV among the AAs measured in *M. edulis* adductor muscles was 2.81. Coefficient of variations were also calculated for each AA and then averaged by site to assess the amount of variability between samples. These values ranged from 2.01 to 5.59; n=8. Samples from Sandy Cove had the lowest coefficient of variation (2.01), while samples from Causeway Road had the highest variability (5.59).

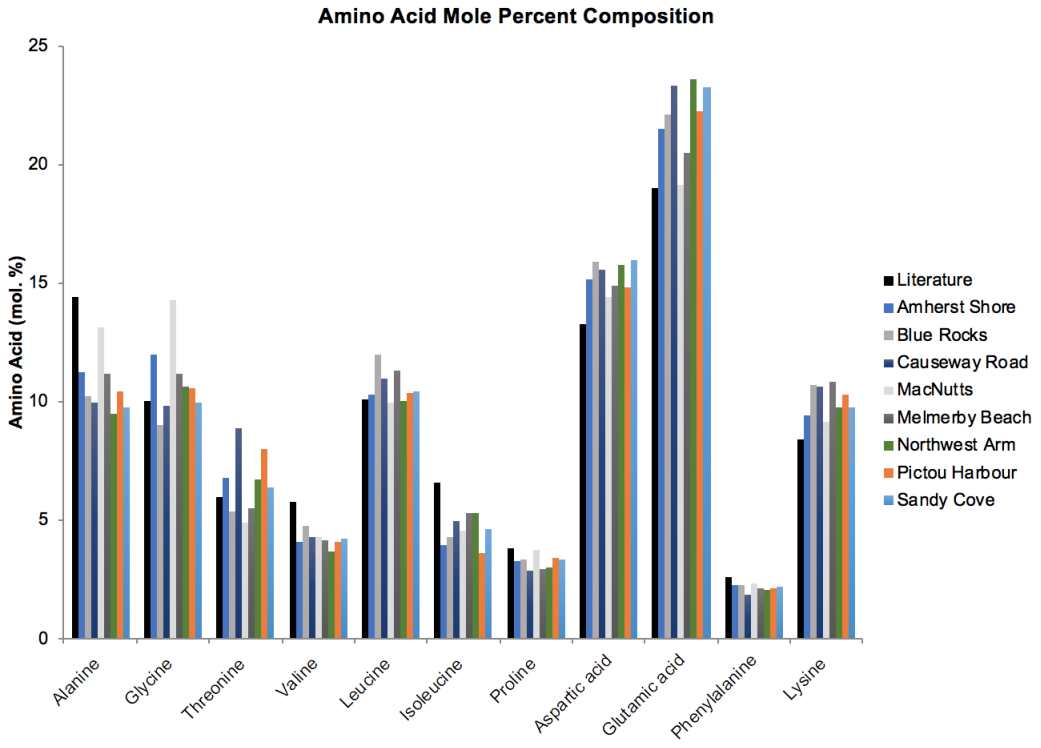

Figure 15: Amino acid mole percent composition of individual AAs averaged by site, along with published values of *M. edulis* Wilbur & Yonge (2013).

3.3.2 CSIA-AA Weighted Averages

Bulk δ^{15}N represents all $\delta^{15}N_{AA}$ values weighted by their respective molar abundances within samples of organic matter (Table 6). This relationship is described in Figure 16, which compares site averages of δ^{15}N values vs the weighted average of the AAs. The relationship does not have a slope of 1 or an r^2 value of of 1 because of a combination of random analytical error and the absence of some AAs, as discussed above. By accounting for these considerations, the overall relationship described is significant because approximately 70% of the bulk δ^{15}N data is represented by the measured AA weight percentages conducted within this study.

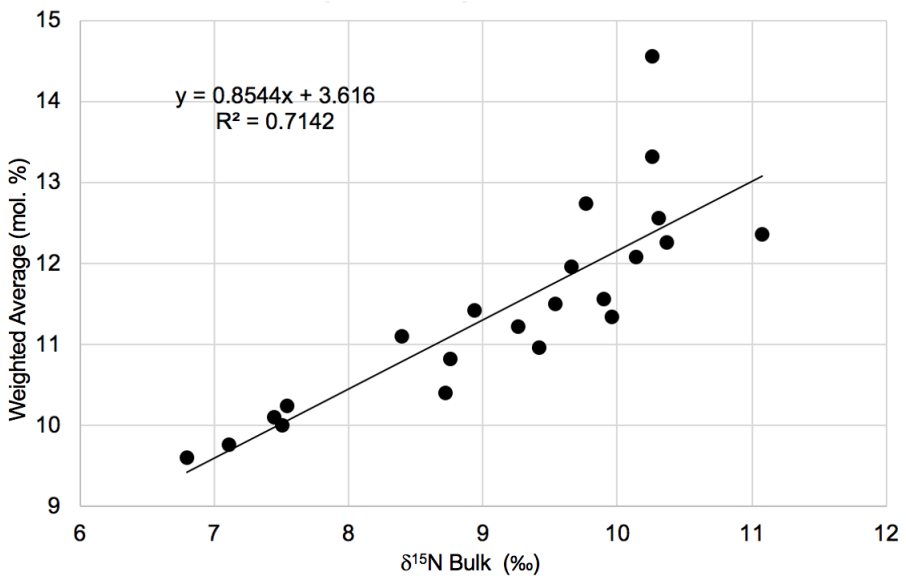

Figure 16: Comparison of CSIA-AA Weighted Average with Measured Bulk δ^{15}N

3.3.3 Overall $\delta^{15}N_{AA}$ Pattern

Figure 16 summarizes the compound specific isotope analysis measurements of average site location amino acid values. Individual amino acid values ranged from -7.5‰ to 18.1‰; n=250. The overall pattern in specimens of *M. edulis* show trophic AAs enriched in ^{15}N, in contrast to the source AAs, and Thr strongly depleted in ^{15}N. This $\delta^{15}N_{AA}$ pattern closely resembles expected patterns of other heterotrophic organisms (e.g., McMahon *et al.* , 2015; Germain *et al.* , 2013; McCarthy *et al.* , 2007). Source AAs (Phe, Lys) ranged from 2.2‰ to 8.9‰ (SD=0.4‰; n=22). The trophic AAs (Glu, Asp, Ala, Leu, Ile, Pro, Val) ranged from 11.0 ± 1.0‰ to 18.1 ± 1.5‰; n=157. In addition to the source and trophic AA groupings, data for two other AAs were analysed. Glycine is an "intermediate" AA that exhibits moderate fractionation with trophic transfer, and had $\delta^{15}N_{Gly}$ values ranged from 3.6 ± 0.8‰ to 9.4 ± 0.8‰; n=22. Threonine is recognized as a "metabolic" AA, which exhibits negative isotopic fractionation in heterotrophic metabolism. $\delta^{15}N_{Thr}$ values ranged from -7.5 ± 2.2‰to 0.1 ± 2.5‰; n=21.

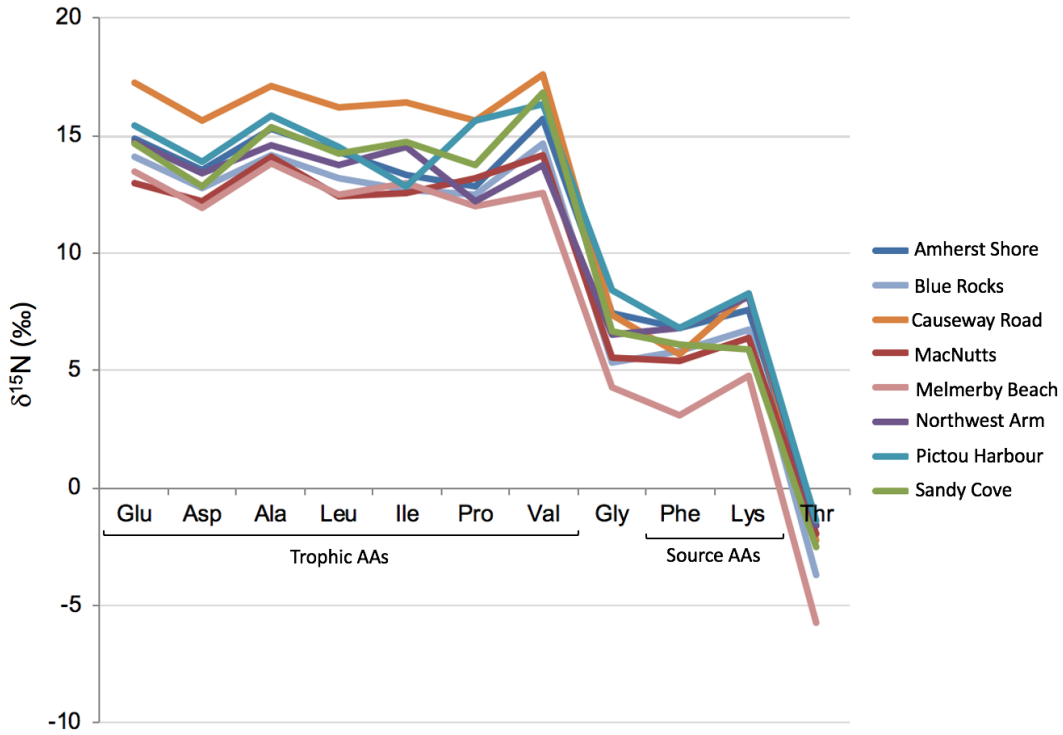

Figure 17: Overall $\delta^{15}N_{AA}$ pattern averaged by site. Trophic and Source AAs are labelled on graph. Glycine (Gly) is considered an "Intermediate AA"" and Threonine (Thr) is a "Metabolic AA."

Table 6: CSIA-AA output.

		Trophic							Intermediate	Source		Metabolic
Site	n	Glu	Asp	Ala	Leu	Ile	Pro	Val	Gly	Phe	Lys	Thr
Amherst Shore	2	14.9(0.5)	13.6(0.8)	15.3(1.3)	14.3(0.8)	13.3(0.7)	12.9(1.2)	15.7(1.9)	7.4(1.2)	6.8(0.1)	7.6(0.1)	-1.6(0.4)
Blue Rocks	3	14.1(0.8)	12.8(0.5)	14.2(0.7)	13.2(0.7)	12.7(1.4)	12.5(1.0)	14.7(0.8)	5.4(0.5)	5.8(1.0)	6.8(0.1)	-3.7(2.2)
Causeway Rd	3	17.3(0.3)	15.6(0.4)	17.1(0.6)	16.2(0.5)	16.4(0.3)	15.6(0.8)	17.6(0.3)	7.4(0.2)	5.7(0.4)	8.3(0.3)	-2.2(0.6)
MacNutts	3	13.0(0.7)	12.2(0.8)	14.1(0.9)	12.4(0.7)	12.6(0.8)	13.2(0.6)	14.2(0.7)	5.6(0.8)	5.4(0.2)	6.4(0.1)	-2.0(0.5)
Melmerby Beach	3	13.4(0.7)	11.9(0.6)	13.8(1.1)	12.5(0.5)	13.0(0.9)	12.0(0.7)	12.6(1.0)	4.3(0.8)	3.1(1.2)	4.8(0.6)	-5.8(2.2)
Northwest Arm	3	14.7(1.6)	13.4(1.2)	14.6(1.7)	13.7(1.8)	14.5(1.9)	12.2(0.4)	13.8(1.6)	6.5(0.4)	6.8(0.9)	8.2(0.1)	-1.6(2.5)
Pictou Harbour	3	15.4(0.3)	13.9(0.2)	15.9(1.6)	14.5(0.6)	12.8(1.6)	15.6(1.8)	16.4(1.5)	8.4(0.8)	6.8(1.0)	8.3(0.4)	-1.4(0.3)
Sandy Cove	3	14.7(0.3)	12.8(0.3)	15.4(0.5)	14.2(0.8)	14.7(0.5)	13.8(0.3)	16.8(0.2)	6.7(0.1)	6.1(0.3)	5.9(0.4)	-2.5(0.2)

3.3.4 $\delta^{15}N_{AA}$ Indices

Average $\delta^{15}N_{AA}$ indices can be found alongside bulk $\delta^{15}N$ and $\delta^{13}C$ in Table 7. $\delta^{15}N_{Phe}$ is considered the best index of baseline of $\delta^{15}N$ primary producer biomass because it does not undergo trophic fractionation. Phe values ranged from 3.1±1.2‰ to 6.8 ± 0.1‰, with the average $\delta^{15}N_{Phe}$ of all sites being 5.8 ± 0.6‰; n=22. Trophic position (TP) calculated using Equation 10 ranged from 1.3 to 2.5, with an average TP of 1.8 ± 0.2. The $\sum V$ parameter is a measure of the degree of heterotrophic microbial alteration and values calculated using Equation 11 ranged from 0.7 to 1.0 (Figure 18). Values of $\sum V$ are plotted with TP on Figure 18, along with data representing fresh algal sources, zooplankton, and detrital particulate organic matter.

Table 7: Summary table of bulk isotope measurements and CSIA-AA indicies.

Site	n	Bulk $\delta^{15}N$	Bulk $\delta^{13}C$	$\delta^{15}N_{Phe}$	TP	$\sum V$
Amherst Shore	2	8.41(0.1)	-21.45(0.2)	6.8(0.1)	1.6(0.1)	0.9(0.1)
Blue Rocks	3	8.42(0.1)	-17.92(0.2)	5.8(1.0)	1.6(0.2)	0.8(0.0)
Causeway Rd	3	9.16(0.3)	-18.18(0.2)	5.7(0.4)	2.1(0.1)	0.7(0.2)
MacNutts	3	6.06(0.4)	-20.32(0.2)	5.4(0.2)	1.6(0.1)	0.7(0.1)
Melmerby Beach	3	5.74(0.3)	-16.04(1.2)	3.1(1.2)	1.9(0.2)	0.7(0.1)
Northwest Arm	3	8.25(1.0)	-19.22(0.4)	6.8(0.9)	1.6(0.3)	0.8(0.3)
Pictou Harbour	3	9.24(0.3)	-19.49(0.1)	6.8(1.0)	1.7(0.1)	1.0(0.1)
Sandy Cove	3	7.21(0.2)	-18.89(0.2)	6.1(0.3)	2.0(0.5)	0.8(0.1)

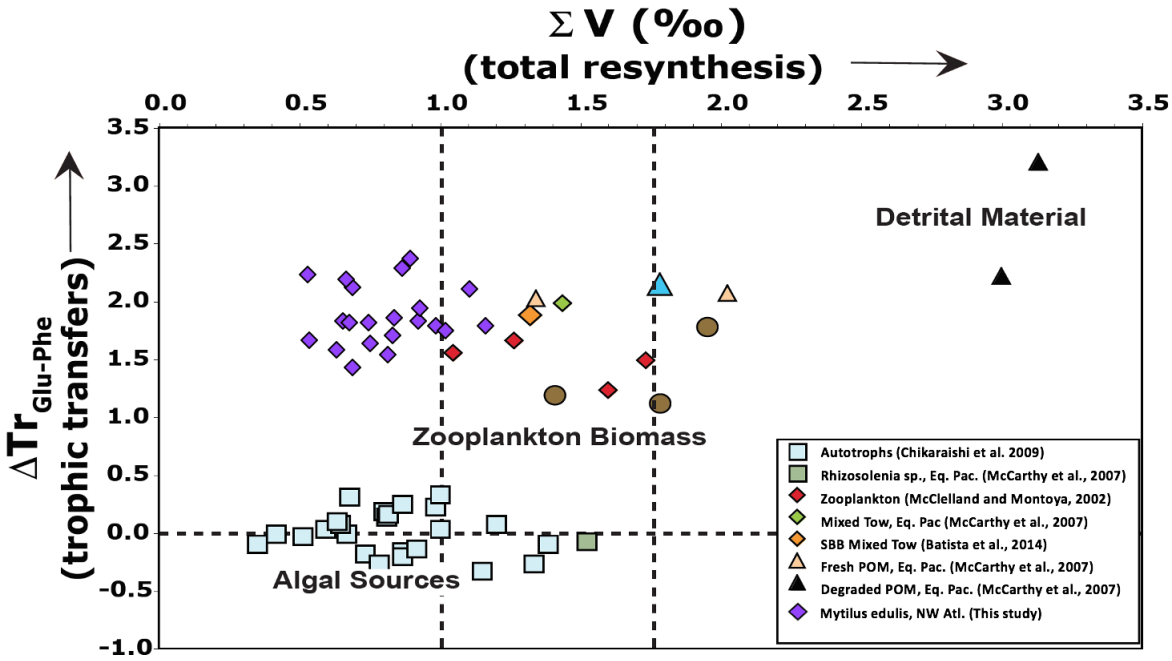

Figure 18: Plot of trophic position index versus the $\sum V$ parameter. Figure adapted from Batista (2016).

3.4 Principle Component Analysis

Principle component analysis (PCA) was conducted on four predictor variables to determine which indicies or measure had the most influence on data distributions. The four predictor variables were $\delta^{15}\mathrm{N}_{Phe}$, $\delta^{13}\mathrm{C}$, TP, $\sum V$. The first two dimensions account for 82.09% of the total variance (55.49% and 26.6%, respectively). The biplot distribution shows that the sample are not clustered in the PCA and do not follow the distribution along any one predictor variable. Note that the coordinate of individuals and variables are not constructed on the same space, so the focus should not be on the absolute positions on the plot but rather the direction of the variables. With the exception of Blue Rocks and Sandy Cove, the majority of the sites loosely follow along the influence of $\delta^{15}\mathrm{N}_{Phe}$ (dimension 1) and $\sum V$ (dimension 2).

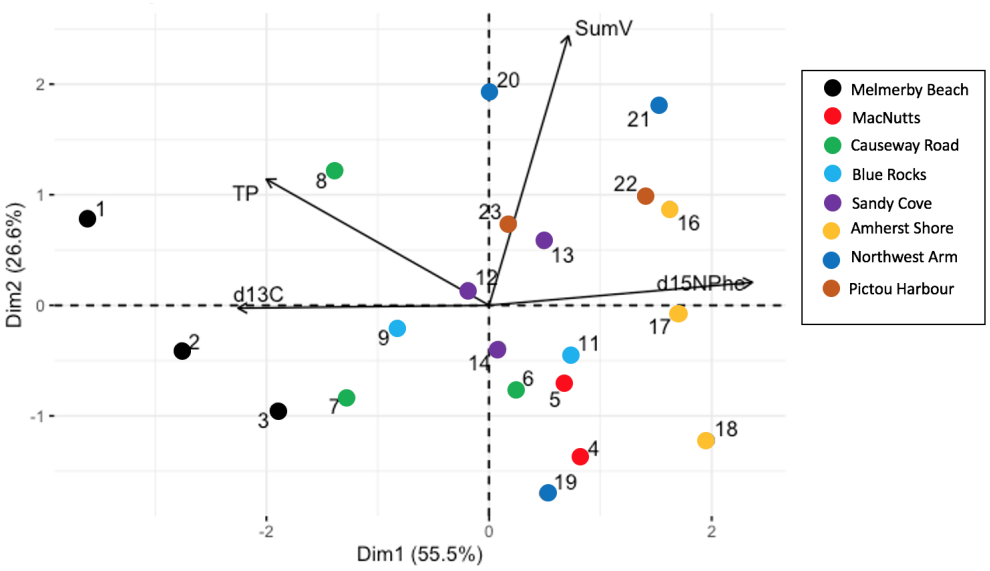

Figure 19: PCA using $\delta^{15}N_{Phe}$, $\delta^{13}C$, TP, $\sum V$ as predictor variables. Sample distribution and variables are not constructed on the same space, therefore, the position of samples shows an individual that is on the same side of a given variable has a high value for this variable, while an individual on the opposite side has a low value or this variable.

4 Discussion

The overall objective of this thesis project was to explore patterns of baseline δ^{15}N variability in coastal NS as recorded in the tissues of a bioindicator organisms. It was hypothesized that the regional background isoscape would be overprinted by localized processes affecting N cycle dynamics, and that these processes were driven by inputs of anthropogenic nitrogen. This study used nutrient data alongside the isotopic δ^{15}N signature preserved in the adductor muscle of *M. edulis* specimen to test the validity of this hypothesis. Nitrogen variability was further assessed using novel CSI-AA approach with traditional bulk δ^{15}N analysis to refine these estimates of baseline δ^{15}N isoscapes independently of trophic fractionation.

4.1 Nutrient Data

Detecting inputs of excess nitrogen to the coastal zone is challenging because many water quality assessment tools are ineffective in dynamic coastal environments. Nutrient concentrations highlight the variability of nitrogen on a regional scale, however, these values act as a temporary refection of the nitrogen behaviour at these locations. Biological uptake of nutrients, particularly following spring and autumn algal blooms, can mask the extent of nutrient pollution (Ryan *et al.* , 2008a). This is highlighted by the fact that NO_3^- concentrations were below the level of detection or quantification at 10 of the 21 sites visited (Table 2), which is to be expected for surface waters collected during the autumn bloom. These low nutrient concentrations precluded calculation of f-ratio or N* at some of the sites. Likewise, tidal flushing may dilute potentially elevated nutrient concentrations, for example at aquaculture sites such as the salmon pens at the MacNutts island site, where the concentrations of NO_3^- (2.79 µM kg^{-1}) and NH4 (1.12 µM kg^{-1}) were within range of published mean values for 31 sites around coastal NS ($NO_3^- = 2.1 \pm 4.5$ µM kg^{-1}; 12.8 ± 28 µM kg^{-1}; Strain & Yeats (1999)).

Nevertheless, some general patterns emerge from the nutrient data. Compared to the more exposed open water sites, dissolved nitrogen concentrations were con-

sistently higher (5.16 – 15.19 µM kg^{-1}) in the Halifax urban area, particularly sites in Bedford Basin (Africville, Birch Cove, Mill Cove) and the Northwest Arm (Cedar Bank, Northwest Arm site; Table 2). These higher NO_3^- concentrations are consistent with generally higher expected fluxes of sewage and industrial effluents of N from urban areas. The Mill Cove site is notable for having both highest concentrations of NO_3^- (15.19 µM kg^{-1}) and NH_4^+ (4.8 µM kg^{-1}). This site receives effluent from the Mill Cove Wastewater Treatment facility in Bedford. The Amherst Shore site also had high concentrations of NO_3^- (13.16 µM kg^{-1}) but the reason for this is not clear as the location is far from any obvious sources of nutrients such as urbanization, agriculture or industry.

Nutrient ratios provided some additional indications of N cycle dynamics. The relationship between NO_3^- concentrations and "pseudo" f-ratio followed a typical logarithmic trend, even after excluding sites where NO_3^- was below the level of detection or quantification (Figure 9). Thus, the sites with lower NO_3^- concentrations (<1 umol/kg; Causeway Road, Tidnish, East Chezzetcook) had lower f-ratios (<0.25), therefore implying a greater reliance on "regenerated" N upon depletion of NO_3^- concentrations (Harrison *et al.* , 1987). The remaining sites with higher NO_3^- (greaterthan 1 µM kg^{-1}) had f-ratios averaging 0.76, thus implying a greater proportion of "new" N, which could be supplied by oceanic upwelling, or by land-based or anthropogenic sources. The N* parameter was not correlated with NO_3^- concentrations; however the overall average N* of -1.3 ± 2.4 (excluding samples below the level of detection of quantification; Table 2) is consistent with net denitrification, which is expected in the more restricted basins with periodic suboxia (Strain & Yeats, 1999) (Haas & Wallace, 2020) (Strain and Yeats, 1999; Haas et al. 2020).

To summarize, the nutrient data provide some indication of nutrient dynamics in the coastal locations considered in this study. However, the data represent only snapshots in time. Repeated sampling over longer timescales would be required to account for temporal variations caused by mixing events, tidal flushing and biological

uptake. Repeat sampling is laborious, thus highlighting the value of bioindicators that integrate biochemical signals over longer periods.

4.2 Mussel Data

Mussels (*M. edulis*) were chosen for this study because they are filter-feeding organisms found along the rocky-intertidal zone of the province's coastline. These mussels are sessile organisms that integrate the isotopic signature of their food source (suspended algae and POM) into their tissues for periods of 3-4 months. Other studies have used primary producers, specifically sessile macroalgae (seaweeds and seagrasses), to measure and map δ^{15}N spatial gradients in the coastal zone of eastern Canada (McIver *et al.* , 2018; Nagel *et al.* , 2018; Howarth *et al.* , 2019), but use of macroalgae may be complicated by growth or nutrient-dependent fractionation effects (Howarth *et al.* , 2019). By contrast, isotopic signatures recorded in mussel adductors smooth out these effects over the 3-4 month turnover times for adductor muscle protein. The use of mussels also mitigates the migratory issues associated with higher level consumers, thus leading to a clearer representation of spatial variability in δ^{15}N.

Specimens of M. edulis were collected in triplicate (wherever possible) from each of the 21 different sites on the Atlantic and Northumberland coasts of NS. Within-site variability in bulk δ^{15}N among triplicate mussel samples was considerably low (mean of standard deviation = 0.56‰), indicating narrow variability within specimens at each site. There was, however, a wide range in bulk values between sites, with δ^{15}N values among all individual specimen of *M. edulis* ranged up to 4.28 $\pm$ 1.27‰; n=61.

The site average bulk δ^{15}N values did not correlate with mussel physiology (Condition Index) or any of the environmental parameters considered (coastal region, environment, f-ratio or N* (Table 3 and 4). The lack of relationship between con-

dition index and bulk δ^{15}N is not surprising because condition index is used as a rough assessment of mussel health. The effect of environmental variables such as temperature, salinity, and food availability may be masked by the intrinsic relationship between CI and the reproductive cycle of the mussels (Filgueira *et al.* , 2013).

There was a significant difference in site average $\delta^{15}N_{bulk}$ between sites without a collection ban (mean δ^{15}N = 8.51 ± 0.7 ‰, n = 10) and with a collection ban (mean δ^{15}N = 9.47 ± 0.7 ‰, n = 7). The collection ban was used to measure water quality and is based on fecal coliform monitoring data gathered from the Canadian Shellfish Sanitation Program (CSSP 2016). From 2005 to 2015, the fecal coliform counts from CSSP monitoring stations located less than 500 m away from seagrass beds were assessed for water quality contamination according to thresholds set by Environment Canada. Coliform counts were used because it is associated with reduced water quality, decreased oxygen, and are often indicative of disease-causing pathogens in coastal shellfish (Murphy *et al.* , 2019). Fecal coliform counts under 14 MPN 100 mL - 1 were considered uncontaminated and would allow that location to remain open for shellfish harvesting. The bulk δ^{15}N versus the collection ban was statistically significant (P = 0.016) which suggest that the bulk δ^{15}N in the mussel tissues are a direct reflection of their environmental conditions. This implication can be made because the collection ban is based on sanitary and bacteriological water quality conditions determined by Environment Canada. *M. edulis* specimen are therefore reliable bionidicator organisms that reflect the water quality conditions of their local environment because higher δ^{15}N measured in sites with a collection ban is consistent with higher loads of sewage derived nitrogen at those sites.

Bulk δ^{15}N in animal tissues integrates the combined influences of baseline δ^{15}N of the animal's diet, plus trophic fractionation of approximately 3.4‰ per each successive increase in trophic position (DeNiro & Epstein, 1981). If the measured between-site range in bulk δ^{15}N (4.28‰) was entirely due to trophic effects (i.e. constant baseline δ^{15}N), then the resulting range in trophic position would be greater

than one. This range in trophic position is unlikely because mussels are non-selective filter-feeders that feed at the level of primary consumers (TP 2). The compound-specific isotope data confirm this, as calculated TP values for the samples selected for $\delta^{15}N_{AA}$ analysis averaged 1.8 ± 0.2 (Table 7). Figure 18 shows the distribution of *M. edulis* TP estimates, which lie approximately one trophic position above fresh algae. The *M. edulis* TP values overlap with that for zooplankton, which also feed on algae. Further, TP did not correlate with any of the environmental parameters considered (region, environment, or nutrient ratios), nor with $\delta^{15}N_{Bulk}$ (Table 7). Therefore, it may be concluded that variations in TP account for, at most, only a fraction (<50%) of the variability in bulk $\delta^{15}N$.

In addition to providing precise estimates of TP, the $\delta^{15}N_{AA}$ data were also used to calculate the SumV parameter, which provides and index of microbial degradation in the diet of *M. edulis* (McCarthy *et al.* , 2007). The calculated $\sum V$ values (0.8 ± 0.1; Table 7) overlap with those for fresh algae (Fig:18). Note that $\sum V$ values for zooplankton biomass are higher because it was difficult to separate live zooplankton from zooplankton fecal pellets, which comprise heterotrophic bacteria and their degradation products (Batista, 2016). There was no significant correlation between $\delta^{15}N_{Bulk}$ and the SumV parameter (P = 0.02), which implies that microbial degradation cannot account for variability in bulk $\delta^{15}N$. This is to be expected in the intertidal zone because the suspended organic material that the mussels are feeding on is supplied by relatively new nitrogen sources, which have not been exposed to heterotrophic bacteria for long periods. One factor to consider with this finding, however, is that this is dependant on the time of year as seasonal upwelling may influence the food sources supplied to the coastal zone.

By eliminating or minimizing the apparent influences of TP and microbial degradation ($\sum V$) on the distribution of bulk $\delta^{15}N$, we can now consider the influence of baseline d15N variability. In contrast to the lack of correlation with TP and SumV, the $\delta^{15}N_{Bulk}$ values strongly correlated with all $\delta^{15}N_{AA}$s, trophic and source alike

(average $R^2 = 0.53$; n=8; Appendix B). This result strongly implicates baseline $\delta^{15}N$ variability as a primary control, as changes in baseline $\delta^{15}N$ affect all the $\delta^{15}N$ of all AAs equally. Specimens from Melmerby had the lowest $\delta^{15}N$ across all AAs, while samples from Causeway Road had the highest overall $\delta^{15}N_{AA}$ values (Fig. 17). The overall influence of baseline $\delta^{15}N$ variability is further evident from the principle component analysis (Figure 19). $\delta^{15}N_{Phe}$ was the predictor variable that was the strongest, accounting for the largest percentage (37%) of the loadings along dimension 1 (Fig.19).

The 8 CSIA-AA sites selected among the 21 sample locations provide important environmental context to these variations in baseline values. Samples collected from Melmerby Beach and Pictou Harbour are two locations that highlight the relationship between bulk isotope analysis and CSIA-AA. Melmerby beach is an estuary located on the Northumberand coast of Nova Scotia (Table **??**). The $\delta^{15}N$ values of bulk mussel tissues at Melmerby beach ranged from 6.8‰ to 7.4‰, and $\delta^{15}N$ values for individual amino acids ranged from -3.3‰ to 15.0‰. The average bulk $\delta^{15}N$ value for Melmerby was among the lowest (mean = 7.1‰) of our CSIA sample locations and the measured $\delta^{15}N_{Phe}$ and average source AA values follow this trend. The mean $\delta^{15}N_{Phe}$ for Melmerby beach was 3.1‰Ṫhese low $\delta^{15}N_{Phe}$ suggest the lack of anthropogenic N sources to the region, but may also be impacted by a lack of circulation within this estuarine sample location. This is contrasted by higher $\delta^{15}N$ values measured from Pictou Harbour, approximately 15km away from Melmerby beach (Table **6**). Samples collected from Pictou Harbour had bulk $\delta^{15}N$ values ranging from 9.9‰ to 10.4‰, and $\delta^{15}N$ values for individual amino acids ranged from -1.6‰ to 18.1‰. The average bulk $\delta^{15}N$ values for Pictou were 10.2‰, with the $\delta^{15}N_{Phe}$ values being among the highest at 6.8‰. The relative proximity of these sample locations provides insight to the variations in baseline N because their $\delta^{15}N_{Phe}$ values are almost doubled from Melmerby beach to Pictou Harbour, despite both locations being restricted environments.

Using measured bulk δ^{15}N isotopic values alongside CSIA-AA it becomes possible to estimate baseline variability for all 21 sites, based on the empirical relationship between $\delta^{15}N_{Bulk}$ and $\delta^{15}N_{Phe}$. Figure 20 shows these modelled baseline values for all 21 sample sites. The inset map highlights Bedford Basin, which includes sites from Africville (5.68‰), Birch Cove (6.06‰) and Mill Cove (4.89‰). The map compares the δ^{15}N values measured in water samples that were collected every week for 3 years (Haas & Wallace, 2020). This study highlights the challenges of water sample data and the need for long-standing collection practices, while complimenting the modelled baseline values of this thesis, (Haas & Wallace, 2020). The combined approach of bulk δ^{15}N and CSIA-AA measuremnts in *M. edulis* tissue thus has the potential to accurately identify baseline δ^{15}N values independant of trophic fractionation. As a rapidly evolving technique, CSIA-AA can further the study of marine foodweb ecology by providing more detailed and accurate representations of the biogeochemical interactions of the ocean.

5 Conclusion

Eutrophication and the degradation of coastal aquatic ecosystems is of growing concern among coastal regions. To address this problem, the isotopic signatures of *M. edulis* specimen were used as bioindicators of fundamental nitrogen cycle processes to better understand the nutrient dynamics within the coastal zone of Nova Scotia. The hypothesis that the regional background isoscape would be overprinted by localized processes affecting N cycle dynamics was supported by the local variability in *M. edulis* $\delta^{15}N_{bulk}$ likely reflecting the inputs of nitrogen sources specific to each area. This basis was used to conduct compound-specific isotope analysis to successfully provide the first estimates of baseline δ^{15}N independent of trophic fractionation within coastal Nova Scotia but ongoing work must be done to understand causes of baseline δ^{15}N variability. The difference in δ^{15}N between sites open and closed to shellfish collection highlight the importance of reconstructing baseline δ^{15}N using mussels as a complementary approach to traditional water quality anal-

ysis and other bioindicator approaches in tracking the sources of N loadings in the coastal environment. By using measured spatial distributions of nitrogen isotope values (δ^{15}N) we can continue to infer biological, physical, chemical,and geological processes in the coastal zone but more spatially-dense sampling across known gradients of N loading is required to further develop and validate the approach.

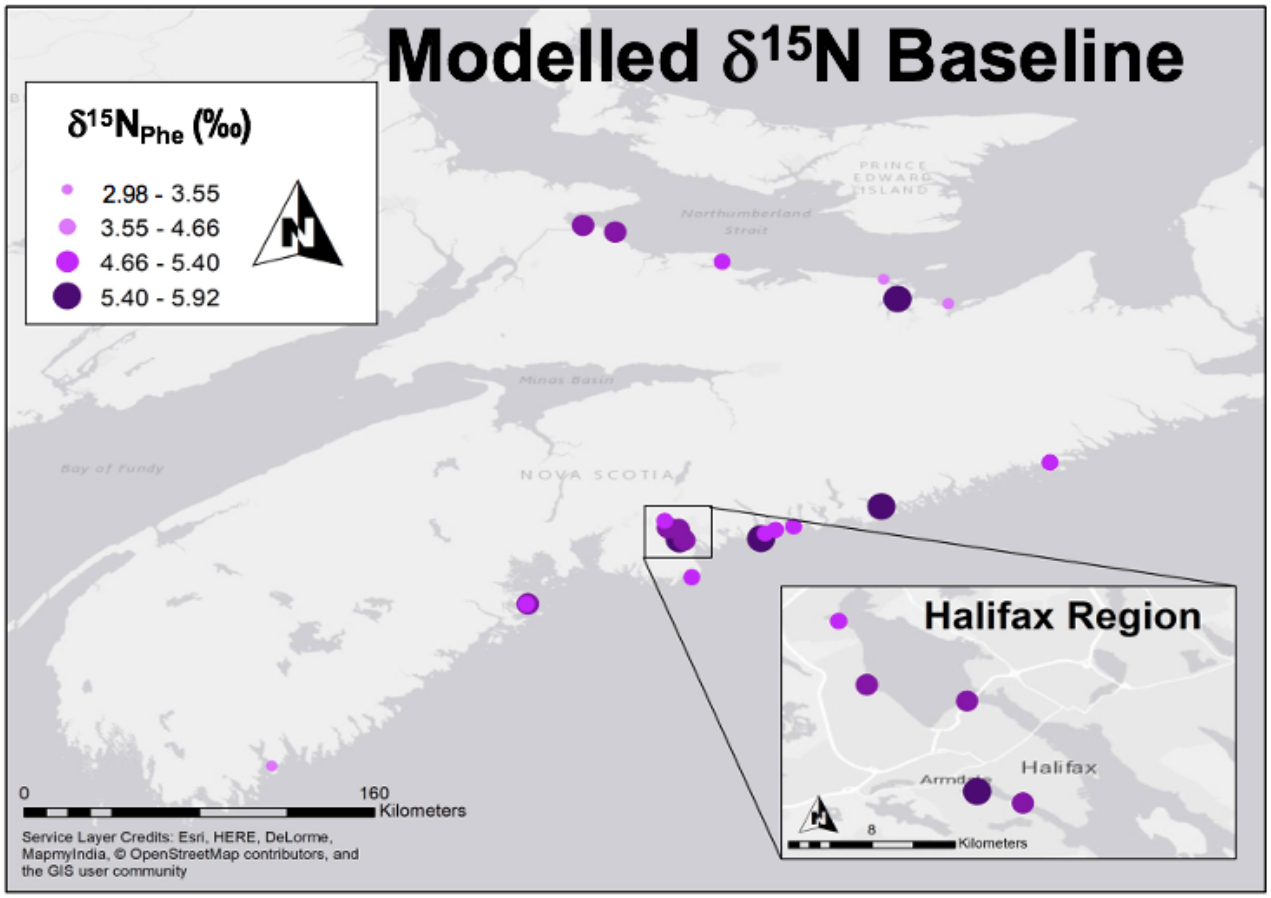

Figure 20: Modelled baseline values for Bedford Basin. Modelled baseline values are depicted in purple while the red circle denotes a high-resolution time-series δ^{15}N measurements of water samples (Haas & Wallace, 2020).

6 Bibliography

Aoyama, M., Anstey, C., Barwell-Clarke, J., Baurand, F., Becker, S., Blum, M., Coverly, S. C., Czobik, E., d'Amico, F., Dahllof, I., *et al.* . 2010. 2008 inter-laboratory comparison study of a reference material for nutrients in seawater.

Batista, F. 2016. *An examination of the marine nitrogen cycle: insights from novel stable nitrogen isotopic approaches*. Ph.D. thesis, UC Santa Cruz.

Bernier, R.Y., J. R., & Moore, A. 2018. *State of the atlantic ocean synthesis report*. Tech. rept. Can. Tech. Rep. Fish. Aquat. Sci. 3167: iii + 149 p.

Bowen, G. J. 2010. Isoscapes: spatial pattern in isotopic biogeochemistry. Annual review of earth and planetary sciences, **38**, 161–187.

Cabana, G., & Rasmussen, J. B. 1996. Comparison of aquatic food chains using nitrogen isotopes. Proceedings of the national academy of sciences, **93**(20), 10844–10847.

Checkley Jr, D. M., & Miller, C. A. 1989. Nitrogen isotope fractionation by oceanic zooplankton. Deep sea research part a. oceanographic research papers, **36**(10), 1449–1456.

Chikaraishi, Y., Ogawa, N. O., Kashiyama, Y., Takano, Y., Suga, H., Tomitani, A., Miyashita, H., Kitazato, H., & Ohkouchi, N. 2009. Determination of aquatic food-web structure based on compound-specific nitrogen isotopic composition of amino acids. Limnology and oceanography: methods, **7**(11), 740–750.

Conley, D. J., Paerl, H. W., Howarth, R. W., Boesch, D. F., Seitzinger, S. P., Havens, K. E., Lancelot, C., & Likens, G. E. 2009. *Controlling eutrophication: nitrogen and phosphorus*.

Coplen, T. B. 1996. New guidelines for reporting stable hydrogen, carbon, and oxygen isotope-ratio data. Geochimica et cosmochimica acta, **60**(17), 3359–3360.

Costanzo, S., O'donohue, M., Dennison, W., Loneragan, N., & Thomas, M. 2001. A new approach for detecting and mapping sewage impacts. Marine pollution bulletin, **42**(2), 149–156.

Craig, H. 1953. The geochemistry of the stable carbon isotopes. Geochimica et cosmochimica acta, **3**(2-3), 53–92.

Crosby, M. 1990. A review and evaluation of bivalve condition index methodologies with a suggested standard method. J shellfish res, **9**, 233–237.

Dalrymple, R. W., Knight, R. J., & Lambiase, J. J. 1978. Bedforms and their hydraulic stability relationships in a tidal environment, bay of fundy, canada. Nature, **275**(5676), 100–104.

Dalsgaard, T., Thamdrup, B., & Canfield, D. E. 2005. Anaerobic ammonium oxidation (anammox) in the marine environment. Research in microbiology, **156**(4), 457–464.

Deborde, J., Anschutz, P., Auby, I., Glé, C., Commarieu, M.-V., Maurer, D., Lecroart, P., & Abril, G. 2008. Role of tidal pumping on nutrient cycling in a temperate lagoon (arcachon bay, france). Marine chemistry, **109**(1-2), 98–114.

DeNiro, M. J., & Epstein, S. 1978. Influence of diet on the distribution of carbon isotopes in animals. Geochimica et cosmochimica acta, **42**(5), 495–506.

DeNiro, M. J., & Epstein, S. 1981. Influence of diet on the distribution of nitrogen isotopes in animals. Geochimica et cosmochimica acta, **45**(3), 341–351.

Diaz, R. J., & Rosenberg, R. 2008. Spreading dead zones and consequences for marine ecosystems. science, **321**(5891), 926–929.

Dugdale, R., & Goering, J. 1967. Uptake of new and regenerated forms of nitrogen in primary productivity 1. Limnology and oceanography, **12**(2), 196–206.

Dyke, A., & Prest, V. 1987. Late wisconsinan and holocene history of the laurentide ice sheet. Géographie physique et quaternaire, **41**(2), 237–263.

Eppley, R. W., & Peterson, B. J. 1979. Particulate organic matter flux and planktonic new production in the deep ocean. Nature, **282**(5740), 677–680.

Falkowski, P. G. 1997. Evolution of the nitrogen cycle and its influence on the biological sequestration of co 2 in the ocean. Nature, **387**(6630), 272–275.

Filgueira, R., Comeau, L., Landry, T., Grant, J., Guyondet, T., & Mallet, A. 2013. Bivalve condition index as an indicator of aquaculture intensity: a meta-analysis. Ecological indicators, **25**, 215–229.

Fowler, D., Coyle, M., Skiba, U., Sutton, M. A., Cape, J. N., Reis, S., Sheppard, L. J., Jenkins, A., Grizzetti, B., Galloway, J. N., *et al.* . 2013. The global nitrogen cycle in the twenty-first century. Philosophical transactions of the royal society b: Biological sciences, **368**(1621), 20130164.

Francis, C. A., Roberts, K. J., Beman, J. M., Santoro, A. E., & Oakley, B. B. 2005. Ubiquity and diversity of ammonia-oxidizing archaea in water columns and sediments of the ocean. Proceedings of the national academy of sciences, **102**(41), 14683–14688.

Fry, B. 2006. *Stable isotope ecology*. Vol. 521. Springer.

García-Sanz, T., Ruiz-Fernández, J., Ruiz, M., García, R., González, M., & Pérez, M. 2010. An evaluation of a macroalgal bioassay tool for assessing the spatial extent of nutrient release from offshore fish farms. Marine environmental research, **70**(2), 189–200.

Gardner, M., Fraser, R., Milloy, M., & Frost, J. 2005. *Economic value of the nova scotia ocean sector*. Nova Scotia Fisheries Sector Council.

Garrett, C. 1972. Tidal resonance in the bay of fundy and gulf of maine. Nature, **238**(5365), 441–443.

Germain, L. R., Koch, P. L., Harvey, J., & McCarthy, M. D. 2013. Nitrogen isotope fractionation in amino acids from harbor seals: implications for compound-specific trophic position calculations. Marine ecology progress series, **482**, 265–277.

Graham, B. S., Koch, P. L., Newsome, S. D., McMahon, K. W., & Aurioles, D. 2010. Using isoscapes to trace the movements and foraging behavior of top predators in oceanic ecosystems. *Pages 299–318 of: Isoscapes*. Springer.

Gran, H. H., & Braarud, T. 1935. A quantitative study of the phytoplankton in the bay of fundy and the gulf of maine (including observations on hydrography, chemistry and turbidity). Journal of the biological board of canada, **1**(5), 279–467.

Gruber, N. 2004. The dynamics of the marine nitrogen cycle and its influence on atmospheric co 2 variations. *Pages 97–148 of: The ocean carbon cycle and climate*. Springer.

Gruber, N., & Sarmiento, J. L. 1997. Global patterns of marine nitrogen fixation and denitrification. Global biogeochemical cycles, **11**(2), 235–266.

Haas, Sebastian, B. M. R. J. L. T. K. S. R., & Wallace, D. 2020. *Unusual nitrification patterns in a eutrophic coastal basin analyzed by geochemical, isotopic and microbiological data from a highly-resolved in situ time series.*

Harrison, W., Platt, T., & Lewis, M. R. 1987. f-ratio and its relationship to ambient nitrate concentration in coastal waters. Journal of plankton research, **9**(1), 235–248.

Hawkins, A., Bayne, B., Day, A., & Denton, E. J. 1986. Protein turnover, physiological energetics and heterozygosity in the blue mussel, mytilus edulis: the basis of variable age-specific growth. Proceedings of the royal society of london. series b. biological sciences, **229**(1255), 161–176.

Heaton, T. H. 1986. Isotopic studies of nitrogen pollution in the hydrosphere and atmosphere: a review. Chemical geology: Isotope geoscience section, **59**, 87–102.

Hobson, K., Van Wilgenburg, S., Wassenaar, L., Powell, R., Still, C., & Craine, J. 2012. A multi-isotope (δ13c, δ15n, δ2h) feather isoscape to assign afrotropical migrant birds to origins. Ecosphere, **3**(5), 1–20.

Howarth, L., Filgueira, R., Jiang, D., Koepke, H., Frame, M., Buchwald, C., Finnis, S., Chopin, T., Costanzo, S., & Grant, J. 2019. Using macroalgal bioindicators to map nutrient plumes from fish farms and other sources at a bay-wide scale. Aquaculture environment interactions, **11**, 671–684.

Hydes, D., Aoyama, M., Aminot, A., Bakker, K., Becker, S., Coverly, S., Daniel, A., Dickson, A., Grosso, O., Kerouel, R., *et al.* . 2010. Determination of dissolved nutrients (n, p, si) in seawater with high precision and inter-comparability using gas-segmented continuous flow analysers.

Kendall, C. 1998. Tracing nitrogen sources and cycling in catchments. *Pages 519–576 of: Isotope tracers in catchment hydrology*. Elsevier.

Kranck, K. 1972a. Geomorphological development and post-pleistocene sea level changes, northumberland strait, maritime provinces. Canadian journal of earth sciences, **9**(7), 835–844.

Kranck, K. 1972b. Tidal current control of sediment distribution in northumberland strait, maritime provinces. Journal of sedimentary research, **42**(3), 596–601.

LeBlanc, C., Bourbonniere, R., Schwarcz, H., & Risk, M. 1989. Carbon isotopes and fatty acids analysis of the sediments of negro harbour, nova scotia, canada. Estuarine, coastal and shelf science, **28**(3), 261–276.

Macko, S. A., Estep, M. L. F., Engel, M. H., & Hare, P. 1986. Kinetic fractionation of stable nitrogen isotopes during amino acid transamination. Geochimica et cosmochimica acta, **50**(10), 2143–2146.

Mann, R. 1978. A comparison of morphometric, biochemical and physiological indexes of condition in marine bivalve molluscs. Energy and environmental stress in aquatic systems, 484–497.

Mariotti, A., Mariotti, F., Champigny, M.-L., Amarger, N., & Moyse, A. 1982. Nitrogen isotope fractionation associated with nitrate reductase activity and uptake of no3- by pearl millet. Plant physiology, **69**(4), 880–884.

McCarthy, M. D., Benner, R., Lee, C., & Fogel, M. L. 2007. Amino acid nitrogen isotopic fractionation patterns as indicators of heterotrophy in plankton, particulate, and dissolved organic matter. Geochimica et cosmochimica acta, **71**(19), 4727–4744.

McClelland, J. W., & Montoya, J. P. 2002. Trophic relationships and the nitrogen isotopic composition of amino acids in plankton. Ecology, **83**(8), 2173–2180.

McClelland, J. W., Valiela, I., & Michener, R. H. 1997. Nitrogen-stable isotope signatures in estuarine food webs: A record of increasing urbanization in coastal watersheds. Limnology and oceanography, **42**(5), 930–937.

McCutchan Jr, J. H., Lewis Jr, W. M., Kendall, C., & McGrath, C. C. 2003. Variation in trophic shift for stable isotope ratios of carbon, nitrogen, and sulfur. Oikos, **102**(2), 378–390.

McGrath, T., Cronin, M., Kerrigan, E., Wallace, D., Gregory, C., Normandeau, C., & McGovern, E. 2019. A rare intercomparison of nutrient analysis at sea: lessons learned and recommendations to enhance comparability of open-ocean nutrient data. Earth system science data, **11**(1), 355–374.

McIver, R., Milewski, I., Loucks, R., & Smith, R. 2018. Estimating nitrogen loading and far-field dispersal potential from background sources and coastal finfish aquaculture: a simple framework and case study in atlantic canada. Estuarine, coastal and shelf science, **205**, 46–57.

McIver, R. 2015. Quantifying nitrogen loading and corresponding eutrophication symptoms in 7 bays in eastern new brunswick, canada.

McMahon, K. W., Polito, M. J., Abel, S., McCarthy, M. D., & Thorrold, S. R. 2015. Carbon and nitrogen isotope fractionation of amino acids in an avian marine predator, the gentoo penguin (pygoscelis papua). Ecology and evolution, **5**(6), 1278–1290.

Murphy, G. E., Wong, M. C., & Lotze, H. K. 2019. A human impact metric for coastal ecosystems with application to seagrass beds in atlantic canada. Facets, **4**(1), 210–237.

Nagel, E., Murphy, G., Wong, M., & Lotze, H. 2018. *Nitrogen loading rates for twenty-one seagrass inhabited bays in nova scotia, canada*. Department of Fisheries and Oceans.

Needoba, J. A., Waser, N., Harrison, P., & Calvert, S. 2003. Nitrogen isotope fractionation in 12 species of marine phytoplankton during growth on nitrate. Marine ecology progress series, **255**, 81–91.

Ohkouchi, N., Chikaraishi, Y., Close, H. G., Fry, B., Larsen, T., Madigan, D. J., McCarthy, M. D., McMahon, K. W., Nagata, T., Naito, Y. I., *et al.* . 2017. Advances in the application of amino acid nitrogen isotopic analysis in ecological and biogeochemical studies. Organic geochemistry, **113**, 150–174.

Owens, N. 1988. Natural variations in 15n in the marine environment. *Pages 389–451 of: Advances in marine biology*, vol. 24. Elsevier.

Peterson, B. J., & Fry, B. 1987. Stable isotopes in ecosystem studies. Annual review of ecology and systematics, **18**(1), 293–320.

Popp, B. N., Graham, B. S., Olson, R. J., Hannides, C. C., Lott, M. J., López-Ibarra, G. A., Galván-Magaña, F., & Fry, B. 2007. Insight into the trophic ecology of yellowfin tuna, thunnus albacares, from compound-specific nitrogen isotope analysis of proteinaceous amino acids. Terrestrial ecology, **1**, 173–190.

Post, D. M. 2002. Using stable isotopes to estimate trophic position: models, methods, and assumptions. Ecology, **83**(3), 703–718.

Ryan, J. P., Gower, J. F., King, S. A., Bissett, W. P., Fischer, A. M., Kudela, R. M., Kolber, Z., Mazzillo, F., Rienecker, E. V., & Chavez, F. P. 2008a. A coastal ocean extreme bloom incubator. Geophysical research letters, **35**(12).

Ryan, S. A., Roff, J. C., & Yeats, P. A. 2008b. Development and application of seasonal indices of coastal-zone eutrophication. Ices journal of marine science, **65**(8), 1469–1474.

Schell, D. M., Barnett, B. A., & Vinette, K. A. 1998. Carbon and nitrogen isotope ratios in zooplankton of the bering, chukchi and beaufort seas. Marine ecology progress series, **162**, 11–23.

Shaw, J., Gareau, P., & Courtney, R. 2002. Palaeogeography of atlantic canada 13–0 kyr. Quaternary science reviews, **21**(16-17), 1861–1878.

Sherwood, O. A., Lehmann, M. F., Schubert, C. J., Scott, D. B., & McCarthy, M. D. 2011. Nutrient regime shift in the western north atlantic indicated by compound-specific δ15n of deep-sea gorgonian corals. Proceedings of the national academy of sciences, **108**(3), 1011–1015.

Sigman, D. M., Altabet, M., McCorkle, D., Francois, R., & Fischer, G. 2000. The δ15n of nitrate in the southern ocean: Nitrogen cycling and circulation in the ocean interior. Journal of geophysical research: Oceans, **105**(C8), 19599–19614.

Sigman, D. M., Karsh, K., & Casciotti, K. 2009. Ocean process tracers: nitrogen isotopes in the ocean.

Silfer, J., Engel, M., Macko, S., & Jumeau, E. 1991. Stable carbon isotope analysis of amino acid enantiomers by conventional isotope ratio mass spectrometry and combined gas chromatography/isotope ratio mass spectrometry. Analytical chemistry, **63**(4), 370–374.

Smith, P. C., & Schwing, F. B. 1991. Mean circulation and variability on the eastern canadian continental shelf. Continental shelf research, **11**(8-10), 977–1012.

Sohm, J. A., Webb, E. A., & Capone, D. G. 2011. Emerging patterns of marine nitrogen fixation. Nature reviews microbiology, **9**(7), 499.

Šraj, L. O., Almeida, M. I. G., Swearer, S. E., Kolev, S. D., & McKelvie, I. D. 2014. Analytical challenges and advantages of using flow-based methodologies for ammonia determination in estuarine and marine waters. Trac trends in analytical chemistry, **59**, 83–92.

Strain, P. M. 2002. Nutrient dynamics in ship harbour, nova scotia. Atmosphere-ocean, **40**(1), 45–58.

Strain, P. M., & Yeats, P. A. 1999. The relationships between chemical measures and potential predictors of the eutrophication status of inlets. Marine pollution bulletin, **38**(12), 1163–1170.

Tan, F., & Strain, P. 1979. Organic carbon isotope ratios in recent sediments in the st lawrence estuary and the gulf of st lawrence. Estuarine and coastal marine science, **8**(3), 213–225.

Vander Zanden, M. J., Vadeboncoeur, Y., Diebel, M. W., & Jeppesen, E. 2005. Primary consumer stable nitrogen isotopes as indicators of nutrient source. Environmental science & technology, **39**(19), 7509–7515.

Vokhshoori, N. L., & McCarthy, M. D. 2014. Compound-specific δ15n amino acid measurements in littoral mussels in the california upwelling ecosystem: a new approach to generating baseline δ15n isoscapes for coastal ecosystems. Plos one, **9**(6).

Wada, E., & Hattori, A. 1978. Nitrogen isotope effects in the assimilation of inorganic nitrogenous compounds by marine diatoms. Geomicrobiology journal, **1**(1), 85–101.

Wada, E., Kadonaga, T., & Matsuo, S. 1975. 15n abundance in nitrogen of naturally occurring substances and global assessment of denitrification from isotopic viewpoint. Geochemical journal, **9**(3), 139–148.

West, J. B., Bowen, G. J., Dawson, T. E., & Tu, K. P. 2009. *Isoscapes: understanding movement, pattern, and process on earth through isotope mapping*. Springer.

Wheeler, P. A., & Kirchman, D. L. 1986. Utilization of inorganic and organic nitrogen by bacteria in marine systems 1. Limnology and oceanography, **31**(5), 998–1009.

Widdows, J., Fieth, P., & Worrall, C. 1979. Relationships between seston, available food and feeding activity in the common mussel mytilus edulis. Marine biology, **50**(3), 195–207.

Wilbur, K. M., & Yonge, C. M. 2013. *Physiology of mollusca*. Vol. 2. Academic Press.

Yokoyama, H., Abo, K., & Ishihi, Y. 2006. Quantifying aquaculture-derived organic matter in the sediment in and around a coastal fish farm using stable carbon and nitrogen isotope ratios. Aquaculture, **254**(1-4), 411–425.

Yuen, K. K. 1974. The two-sample trimmed t for unequal population variances. Biometrika, **61**(1), 165–170.

Appendix A – Google Earth Imagery of Sample Locations

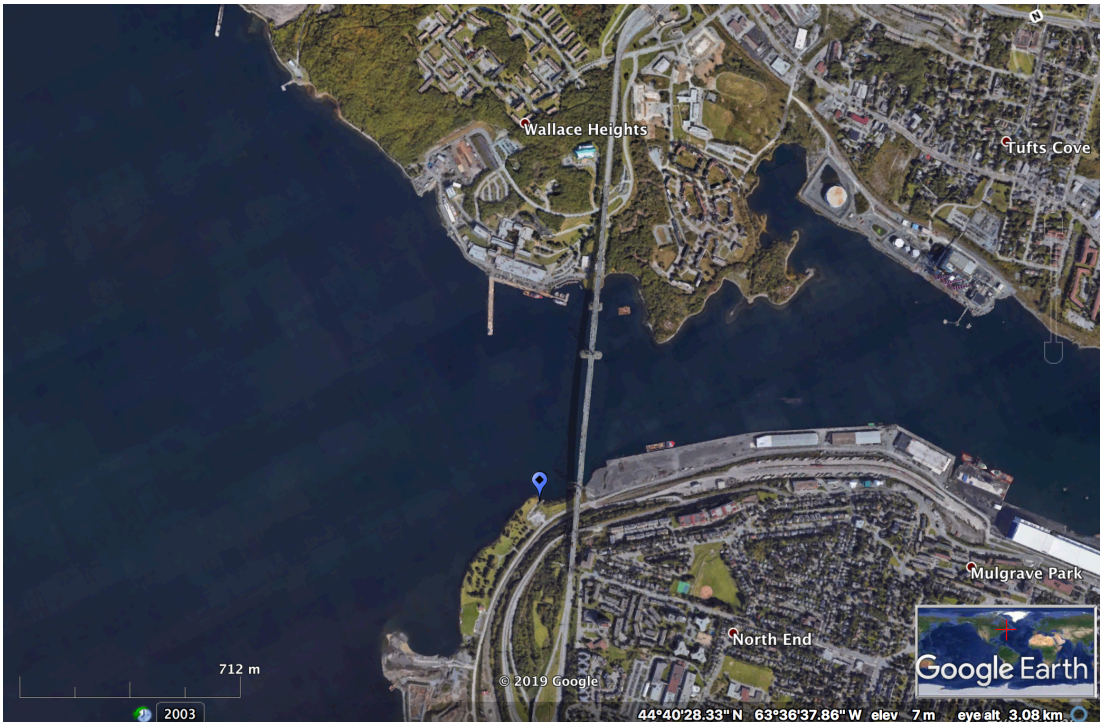

Figure 1: Africville

Figure 2: Amherst

Figure 3: Bedford Basin – from left to right: Mill Cove, Birch Cove, and Africville

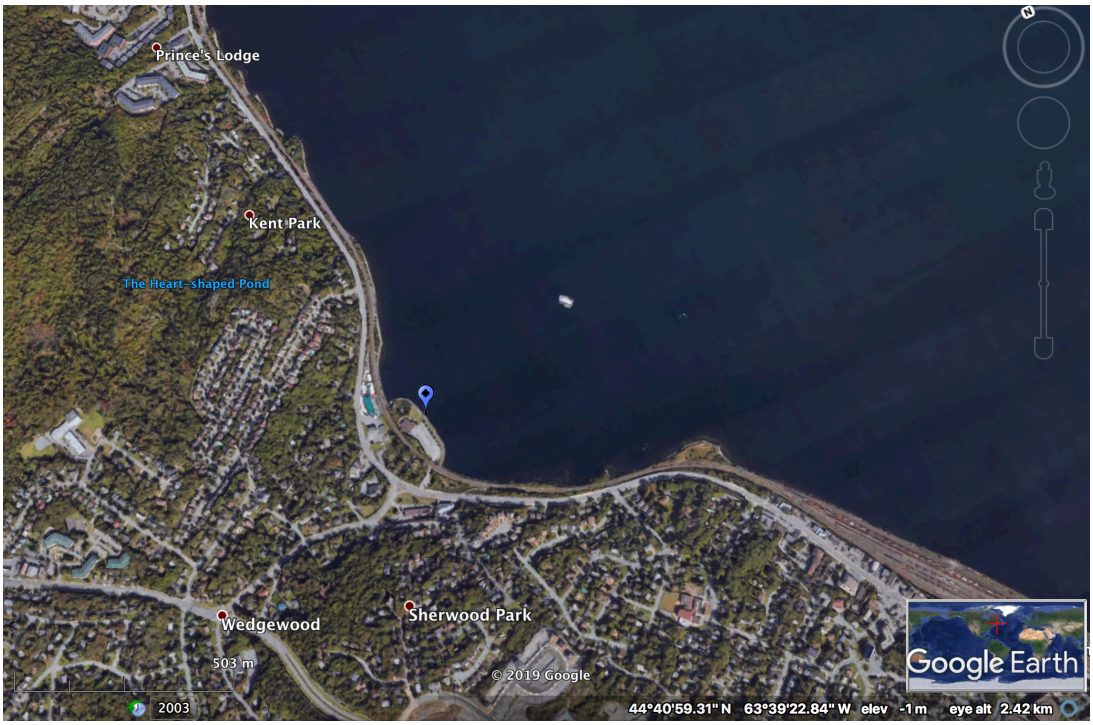

Figure 4: Birch Cove

Figure 5: Blue Rocks

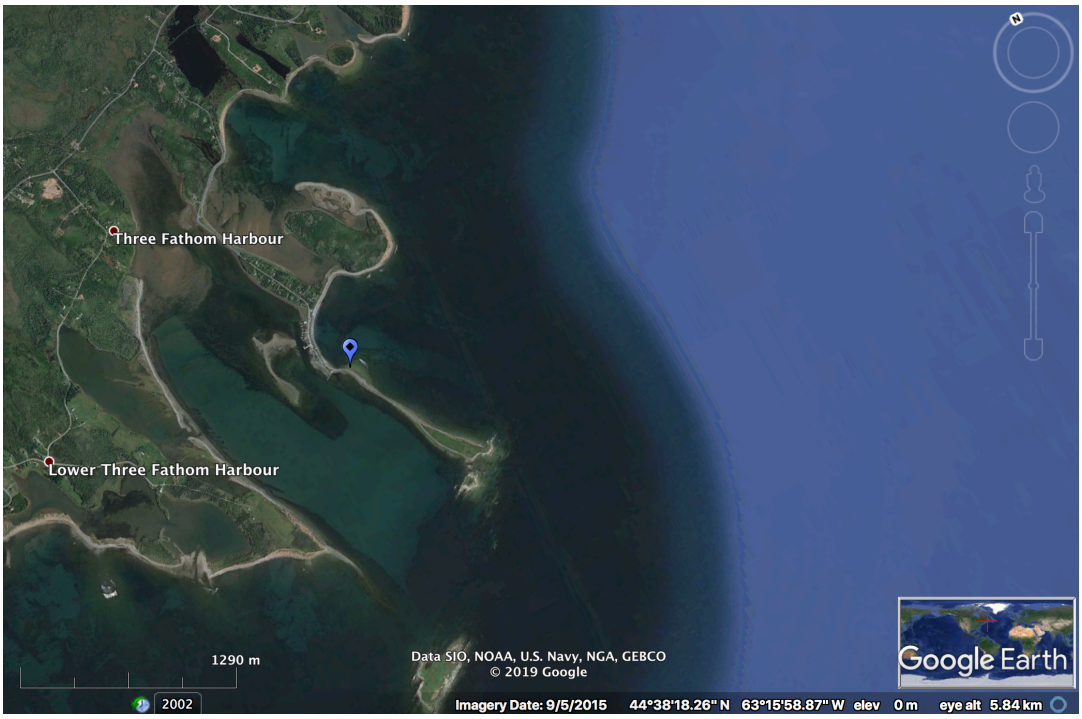

Figure 6: Causeway Road

Figure 7: East Chezzetcook

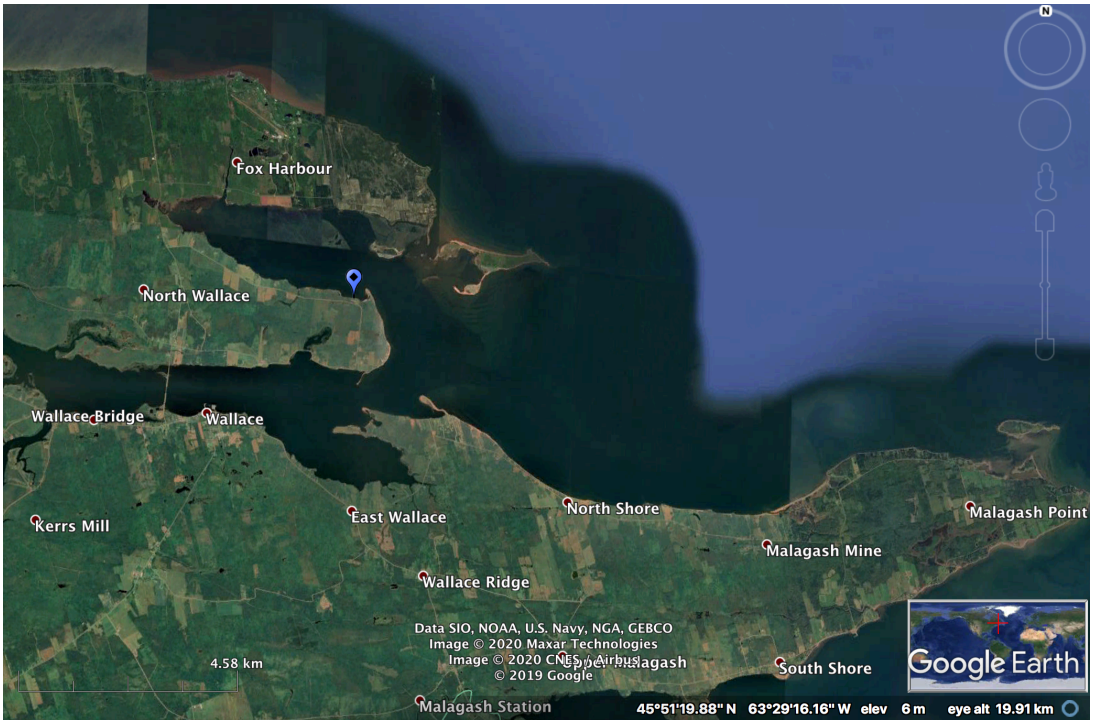

Figure 8: Fox Harbour

Figure 9: MacNutts Island

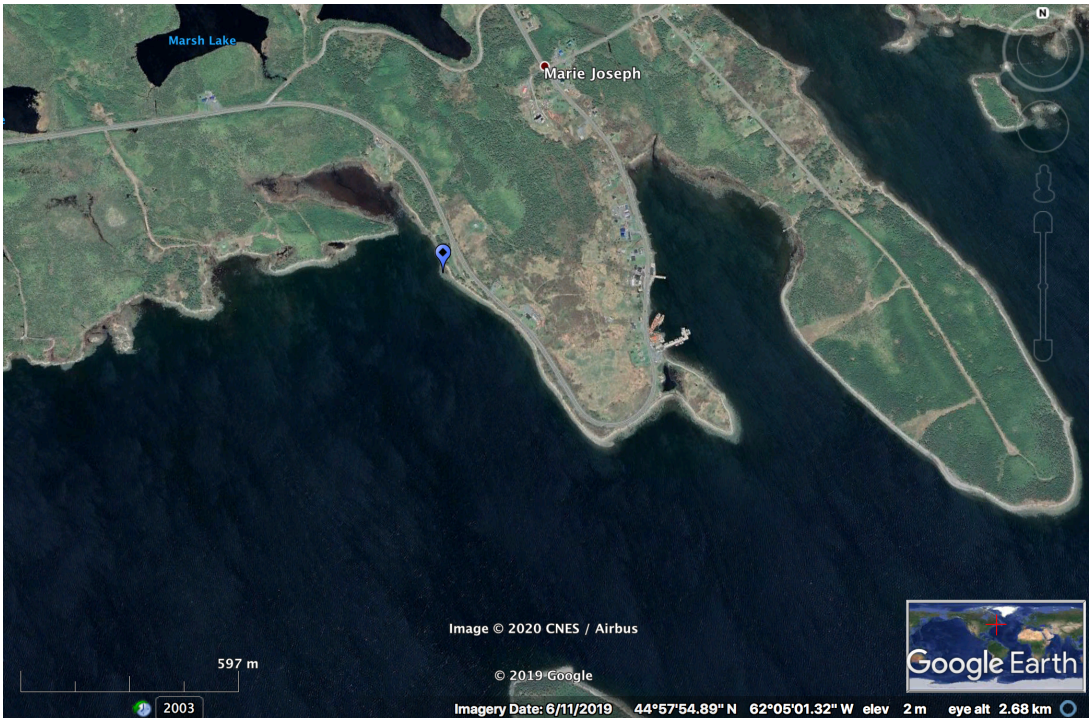

Figure 10: Marie Joseph

Figure 11: Northwest Arm

Figure 12: Martinique

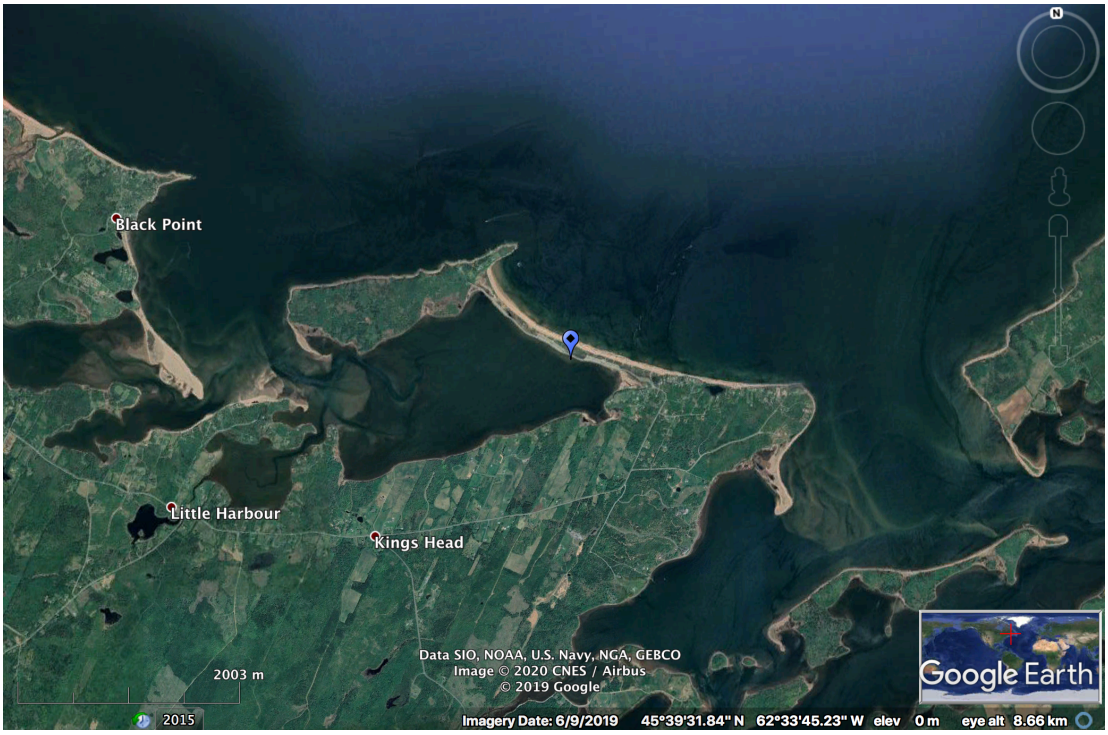

Figure 13: Melmerby Beach

Figure 14: Mill Cove

Figure 15: Norse Cove

Figure 16: Pictou Harbour

Figure 17: Pleasant Paddling

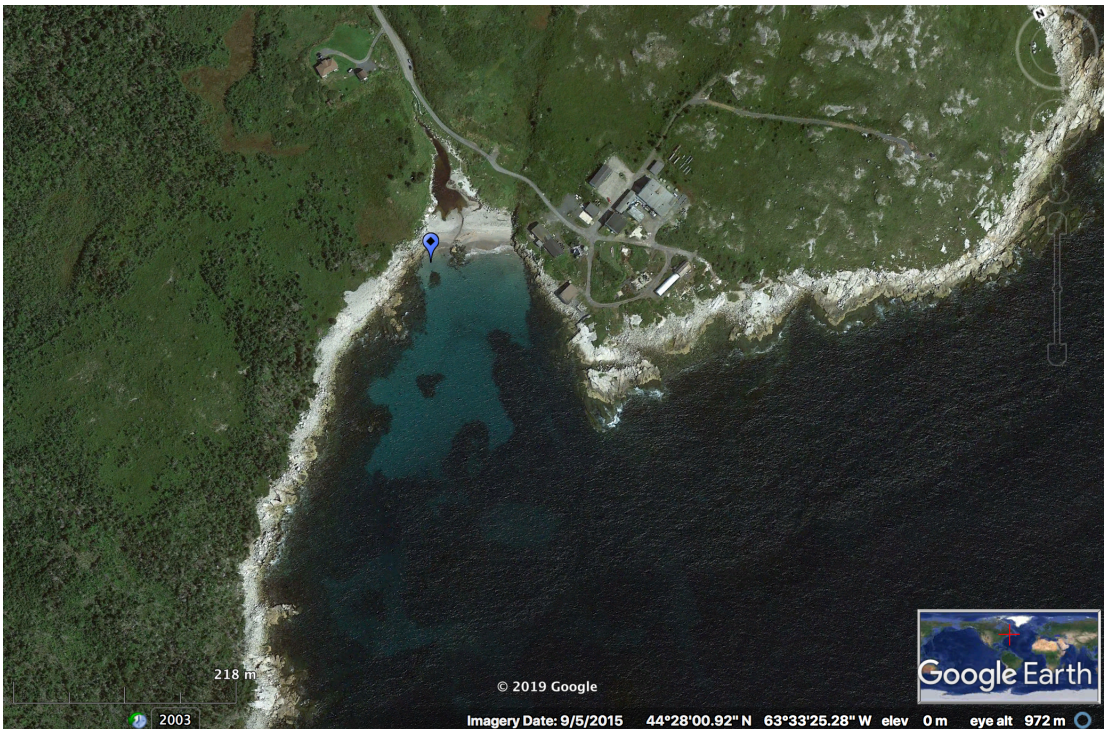

Figure 18: Sandy Cove

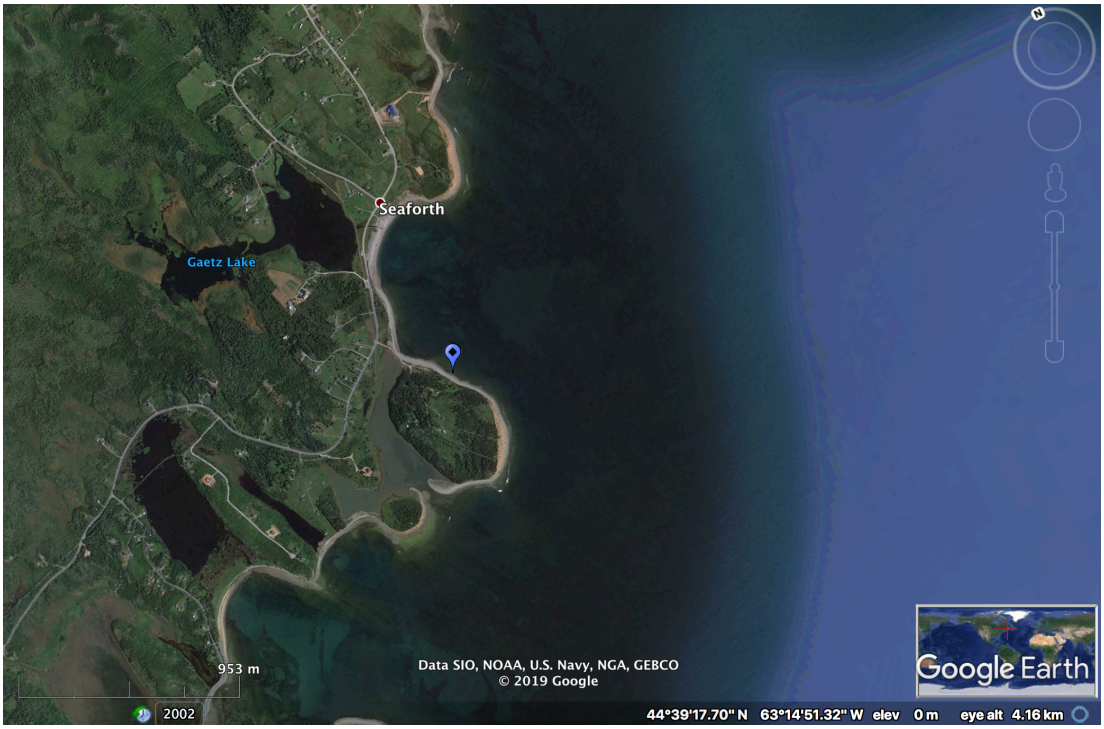

Figure 19: Seaforth

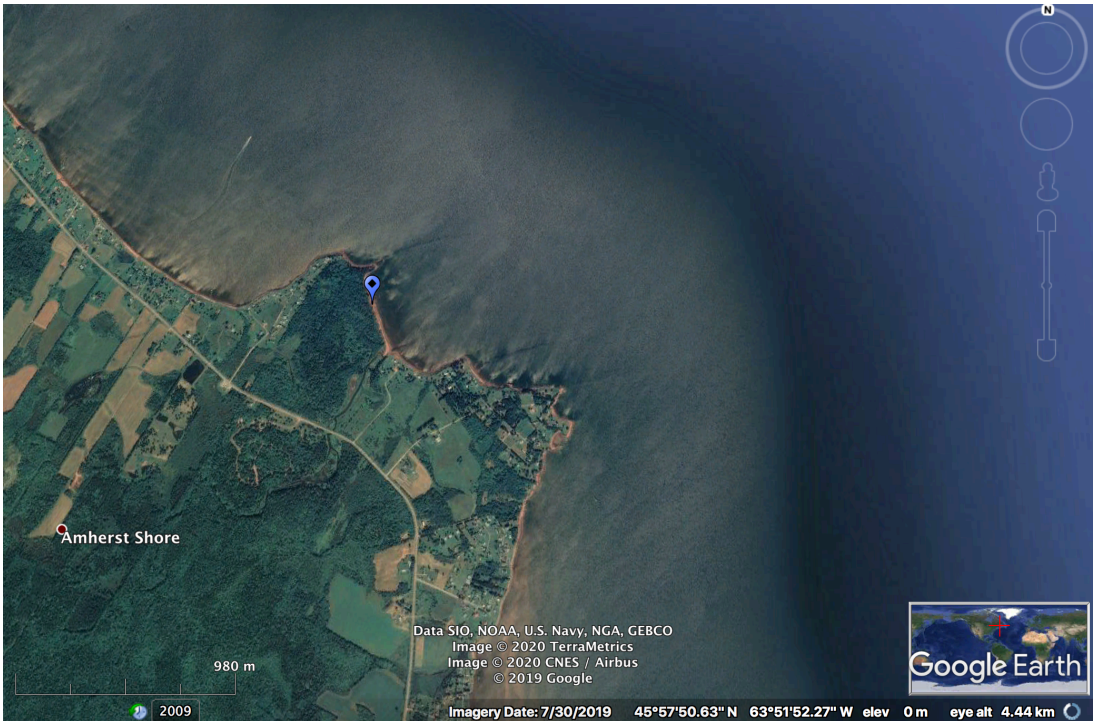

Figure 20: Tidnish

Figure 21: Waterside

Appendix B – Bulk vs Individual AAs

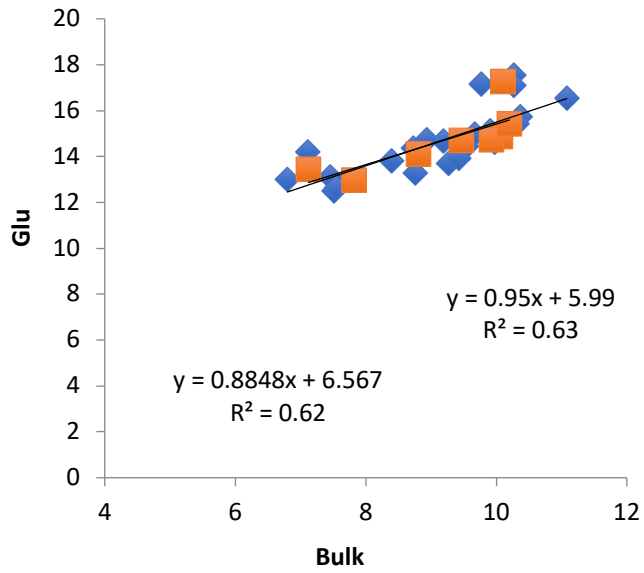

Figure 1: Glutamic Acid (‰) vs Bulk $\delta^{15}N$ (‰). Orange squares are average Glu from the 8 CSIA-AA sites and blue diamonds are all measured $\delta^{15}N_{Glu}$ values measured from the triplicate samples at those 8 sites.

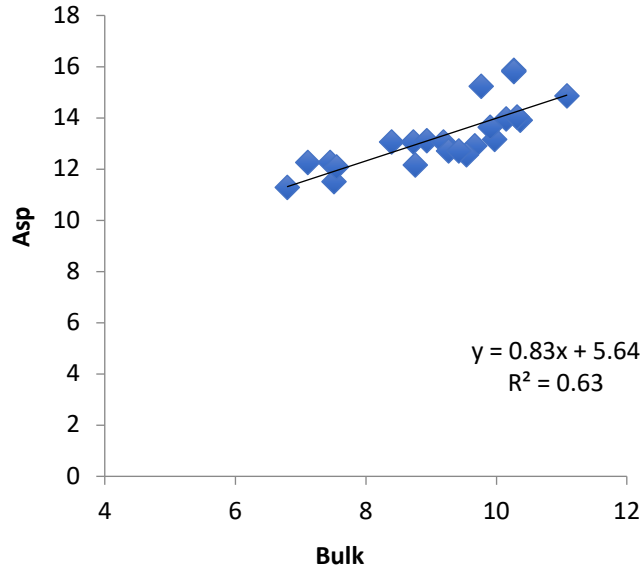

Figure 2: Aspartic Acid (‰) vs Bulk $\delta^{15}N$ (‰)

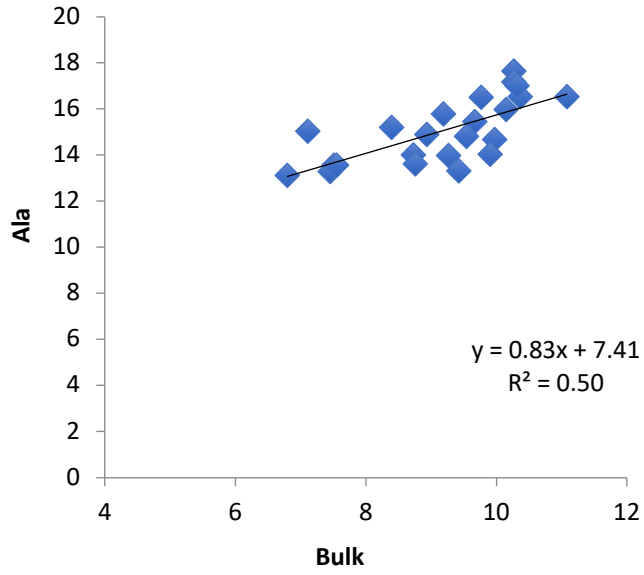

Figure 3: Alanine (‰) vs Bulk $\delta^{15}N$ (‰)

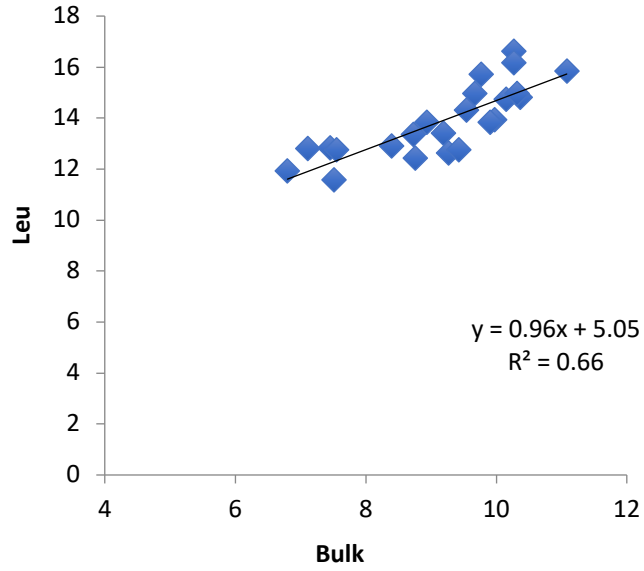

Figure 4: Leucine (‰) vs Bulk $\delta^{15}N$ (‰)

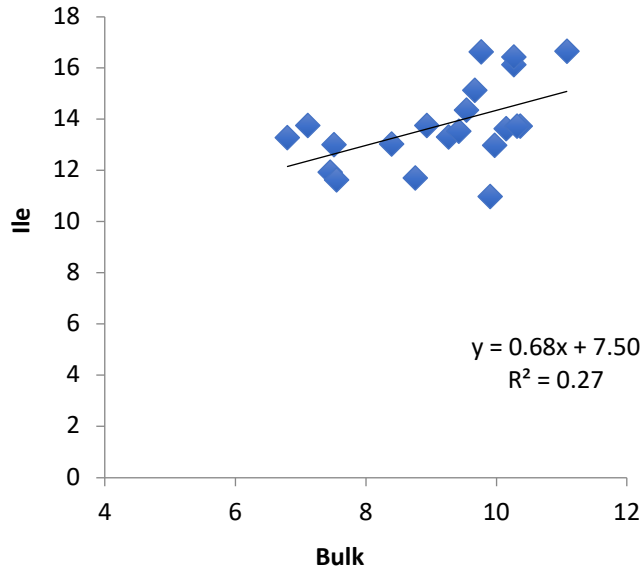

Figure 5: Isoleucine (‰) vs Bulk δ^{15}N (‰)

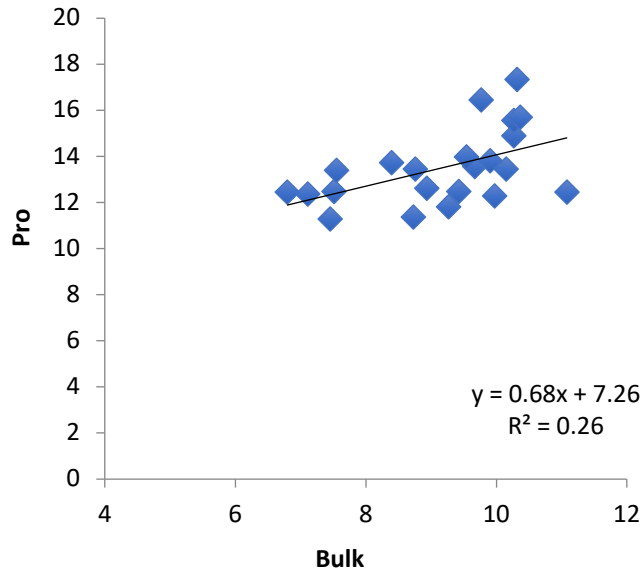

Figure 6: Proline (‰) vs Bulk δ^{15}N (‰)

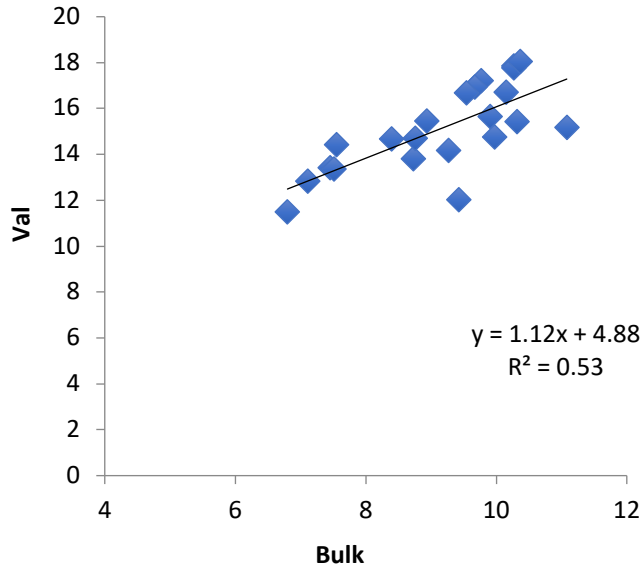

Figure 7: Valine (‰) vs Bulk δ^{15}N (‰)

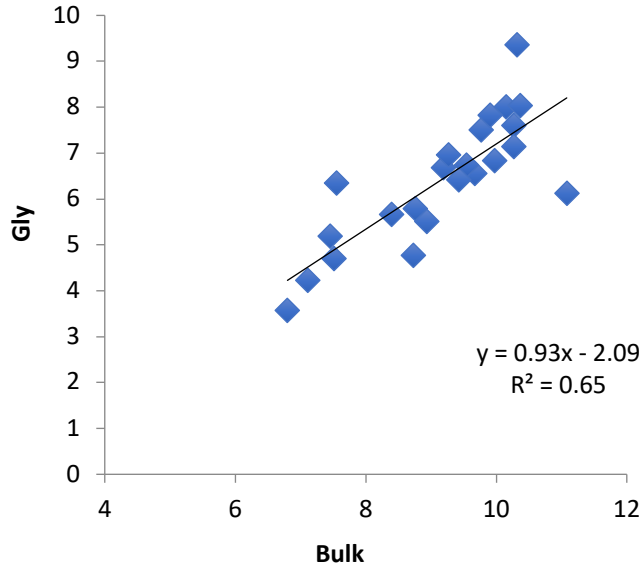

Figure 8: Glycine (‰) vs Bulk δ^{15}N (‰)

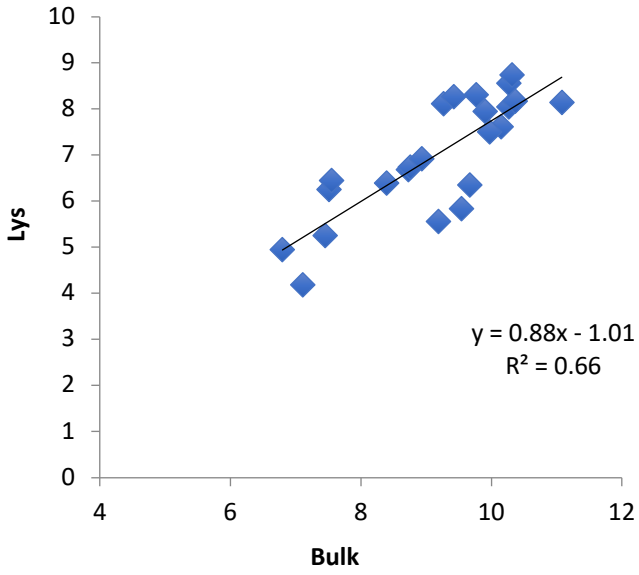

Figure 9: Lysine (‰) vs Bulk $\delta^{15}N$ (‰)

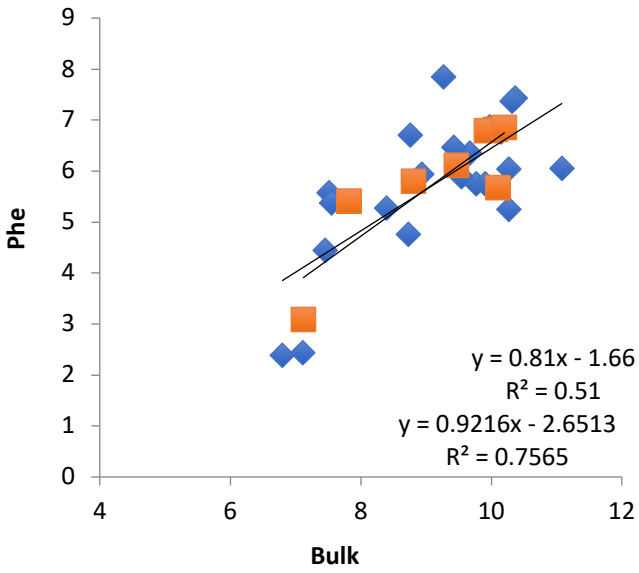

Figure 10: Phenylalanine (‰) vs Bulk $\delta^{15}N$ (‰). Orange squares are average Phe from the 8 CSIA-AA sites and blue diamonds are all measured $\delta^{15}N_{Phe}$ values measured from the triplicate samples at those 8 sites.

Appendix C – Summary of the CSIA-AA Site Averages